USGS
science for a changing world

# A Decade of Geodetic Change at Kīlauea's Summit—Observations, Interpretations, and Unanswered Questions from Studies of the 2008–2018 Halemaʻumaʻu Eruption

Chapter G of
**The 2008–2018 Summit Lava Lake at Kīlauea Volcano, Hawaiʻi**

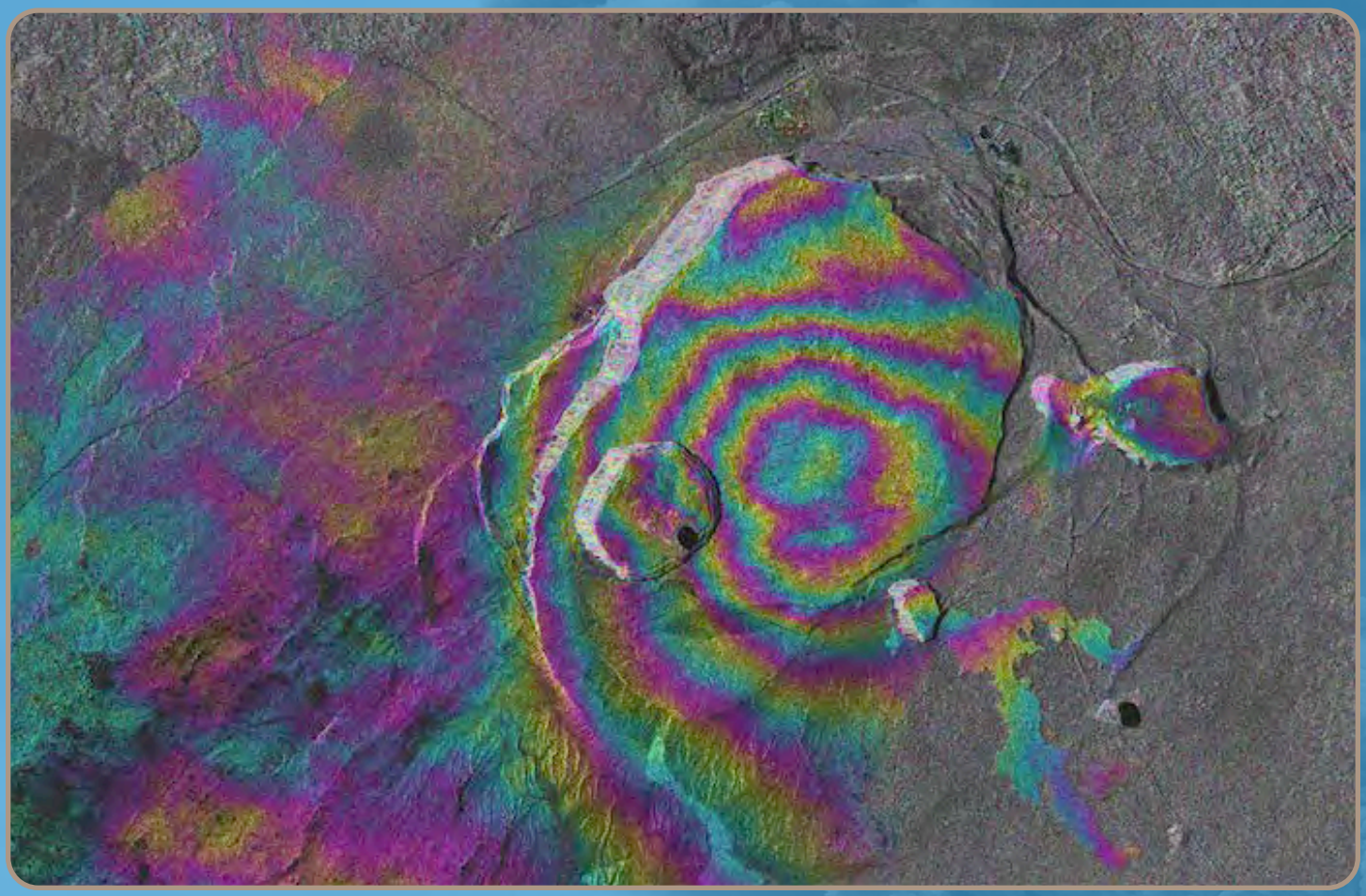

Professional Paper 1867

U.S. Department of the Interior
U.S. Geological Survey

**Cover.** TerraSAR-X interferogram of Kīlauea Caldera spanning April 2 to October 6, 2011. The colored fringes indicate surface deformation—in this case, motion toward the satellite in the center of the caldera, indicating uplift, and away from the satellite in the north part of the caldera, indicating subsidence. A small amount of localized subsidence is also apparent on the rim of the summit eruptive vent, within Halema‘uma‘u. Interferograms like this provided a critical means of monitoring surface deformation throughout the 2008–2018 summit eruption. Background photograph on front and back cover is of a tephra-rich plume rising above Halema‘uma‘u; photograph taken by Gail Ferguson, Hawaiian Volcano Observatory volunteer.

# A Decade of Geodetic Change at Kīlauea's Summit—Observations, Interpretations, and Unanswered Questions from Studies of the 2008–2018 Halemaʻumaʻu Eruption

By Michael P. Poland, Asta Miklius, Ingrid A. Johanson, and Kyle R. Anderson

Chapter G of
**The 2008–2018 Summit Lava Lake at Kīlauea Volcano, Hawaiʻi**
Edited by Matthew Patrick, Tim Orr, Don Swanson, and Bruce Houghton

Professional Paper 1867

**U.S. Department of the Interior**
**U.S. Geological Survey**

U.S. Geological Survey, Reston, Virginia: 2021

For more information on the USGS—the Federal source for science about the Earth, its natural and living resources, natural hazards, and the environment—visit https://www.usgs.gov or call 1–888–ASK–USGS.

For an overview of USGS information products, including maps, imagery, and publications, visit https://store.usgs.gov.



Suggested citation:
Poland, M.P., Miklius, A., Johanson, I.A., and Anderson, K.R., 2021, A decade of geodetic change at Kīlauea's summit—Observations, interpretations, and unanswered questions from studies of the 2008–2018 Halema'uma'u eruption, chap. G *of* Patrick, M., Orr, T., Swanson, D., and Houghton, B., eds., The 2008–2018 summit lava lake at Kīlauea Volcano, Hawai'i: U.S. Geological Survey Professional Paper 1867, 29 p., https://doi.org/10.3133/pp1867G.

ISSN 1044-9612 (print)
ISSN 2330-7102 (online)

# Acknowledgments

We are grateful to our friends and colleagues at the Hawaiian Volcano Observatory (HVO) for their support and encouragement before, during, and after Kīlauea's 10-year-long summit eruption. In particular, we are grateful to the HVO deformation support staff, Maurice Sako and Sarah Conway, who conducted many of the field measurements described in this report, and to HVO's Field Equipment and Instrumentation Team, including Kevan Kamibayashi, Bruce Furukawa, Steven Fuke, CJ Moniz, and Frank Younger, for their work on installing and maintaining continuous geodetic instrumentation in the corrosive environment.

All of the data described in this report were collected within Hawai'i Volcanoes National Park, and we appreciate the collaboration and support of numerous Hawai'i Volcanoes National Park staff over the years in facilitating our monitoring and research efforts.

Interferometric synthetic aperture radar data shown in this report were acquired by TerraSAR-X (German Space Agency), COSMO-SkyMed (Italian Space Agency), and Sentinel-1 (European Space Agency) via the Hawai'i Volcanoes Supersite as established by the Geohazard Supersites and Natural Laboratories initiative. Copernicus Sentinel data used in this report are from 2015.

We would also like to extend our thanks to David Trang, who worked tirelessly to collect GNSS data from the summit; to Jessica Johnson, whose research merged geodetic, seismic, gas, and geologic data to better understand magma storage, transport, and eruption; to Marco Bagnardi, who dedicated himself to developing campaign gravity measurements into a useful monitoring tool; to Daniele Carbone, who provided the expertise needed to establish continuous gravity monitoring; and to numerous volunteers who assisted with field and office assignments related to monitoring the summit eruption, including Flavio Cannavo, Brie Corsa, Devin Cowan, Ryan Ferguson, Shannon Graham, Ashley Gross, Tyler Huth, Rebecca Kramer, Danielle La Marra, Hélène Le Mével, Brian Meyers, Patricia MacQueen, Andrew Mitchell, Camilla Owens, Andy Pitty, Nicole Richter, Kirsten Stephens, Reid Townson, Kelly Wooten, Robin Wylie, Nicky Young, and Jeff Zurek.

Our thanks to reviewers Dan Dzurisin and Tina Neal, whose comments resulted in a much-improved manuscript; to Bob Tilling and Monica Erdman for their expert editing and guidance; to Katie Sullivan for her careful and comprehensive work on the figures in this manuscript; and to Kimber Petersen and Cory Hurd for their design of the layout.

# Contents

## Figures

# Conversion Factors

International System of Units to U.S. customary units

| Multiply | By | To obtain |
|---|---|---|
| | Length | |
| centimeter (cm) | 0.3937 | inch (in.) |
| meter (m) | 3.281 | foot (ft) |
| kilometer (km) | 0.6214 | mile (mi) |
| meter (m) | 1.094 | yard (yd) |
| | Area | |
| square meter ($m^2$) | 10.76 | square foot ($ft^2$) |
| square meter ($m^2$) | 0.0002471 | acre |
| | Volume | |
| cubic meter ($m^3$) | 35.31 | cubic foot ($ft^3$) |
| cubic kilometer ($km^3$) | 0.2399 | cubic mile ($mi^3$) |
| | Flow rate | |
| centimeters per year (cm/yr) | 0.3937 | inches per year (in/yr) |
| meter per second (m/s) | 3.281 | foot per second (ft/s) |
| | Mass | |
| kilogram (kg) | 2.205 | pound avoirdupois (lb) |
| | Density | |
| kilogram per cubic meter ($kg/m^3$) | 0.06242 | pound per cubic foot ($lb/ft^3$) |
| gram per cubic centimeter ($g/cm^3$) | 62.4220 | pound per cubic foot ($lb/ft^3$) |

Temperature in degrees Celsius (°C) may be converted to degrees Fahrenheit (°F) as follows:
°F = (1.8 × °C) + 32.

# Abbreviations

| | |
|---|---|
| DI | deflation-inflation |
| EDM | electronic distance measurement |
| ERZ | East Rift Zone |
| GNSS | Global Navigation Satellite System |
| GPS | Global Positioning System |
| HST | Hawaii Standard TIme |
| HVO | Hawaiian Volcano Observatory |
| InSAR | interferometric synthetic aperture radar |
| LOS | line of sight |
| µGal | microgal |
| RSAM | real-time seismic-amplitude measurement |
| VLP | very long period |

# A Decade of Geodetic Change at Kīlauea's Summit—Observations, Interpretations, and Unanswered Questions from Studies of the 2008–2018 Halema'uma'u Eruption

By Michael P. Poland, Asta Miklius, Ingrid A. Johanson, and Kyle R. Anderson

## Abstract

On March 19, 2008, a small explosion heralded the onset of an extraordinary eruption at the summit of Kīlauea Volcano. The following 10 years provided unprecedented access to an actively circulating lava lake located within a region monitored by numerous geodetic tools, including Global Navigation Satellite System (GNSS), interferometric synthetic aperture radar (InSAR), tilt, and gravity. These datasets revealed a range of processes occurring on widely different timescales. Over years, pressure change within the summit magmatic system, determined from ground deformation and lava-lake surface height, seems to have been governed by broad variations in the rate of magma supply from the mantle to the volcano's shallow magmatic system, as well as changes in the efficiency of East Rift Zone (ERZ) magma transport and eruption. Over weeks to months, intrusions at the summit and along the ERZ, where new eruptive vents commonly formed and intrusions were primed by extension from south-flank motion, were a result of short-term increases in magma supply or waning lava effusion from the ERZ. Waning lava effusion caused magma to back up behind the ERZ eruptive vent all the way to the summit. ERZ intrusions and eruptions caused rapid depressurization of the summit magmatic system, whereas summit intrusions resulted in complex deformation patterns as magma moved to and from two main sub-caldera storage areas. Over hours to days, pressure changes were caused by episodic deflation-inflation (DI) events and possibly small summit intrusions, and deformation of the rim of the summit eruptive vent revealed instabilities that indicated an increased potential for collapse and minor explosive activity. Finally, over timescales of minutes to hours, gas pistoning, summit explosions, very-long-period seismic events, and even the airborne eruptive plume had clear manifestations in geodetic datasets, providing insights into the causes and consequences of those processes. The diversity and quantity of geodetic observations shed important light on this exceptional and well-documented decade-long summit eruption and its accompanying phenomena, yet numerous questions remain about the causal mechanisms, physical processes, and magmatic conditions associated with eruptive and intrusive activity.

## Introduction

The 2008–2018 summit eruption of Kīlauea Volcano, Hawai'i, provided an exceptional opportunity for research and discovery (Patrick and others, 2021). The eruptive vent, inside which an actively circulating lava lake was usually present, was easily accessible and located in the middle of a dense and comprehensive monitoring network within which new equipment could quickly be added. Moreover, this eruption was at a well-studied volcano where a century of research had established a strong framework for understanding the shallow magmatic plumbing system and associated volcanic activity. As a result, an outstanding record of observations was obtained (for example, Patrick and others, 2021) during the eruption, leading to a vast array of detailed insights into magmatic processes ranging from bubble nucleation (for example, Carey and others, 2012, 2013) to the hydraulic connectivity of Kīlauea's extensive magmatic system (for example, Patrick and others, 2019a). The correlation between surface deformation and lava-lake level proved particularly important, providing information on such parameters as the density of the lava lake (Carbone and others, 2013; Poland and Carbone, 2016, 2018), the potential for intrusions and eruptions at the summit and along the volcano's East Rift Zone (ERZ; fig. 1) (Patrick and others, 2015), and the volume of the shallow magmatic system (Anderson and others, 2019).

In this study, we utilize records from numerous types of geodetic sensors to examine a variety of signals related to changes within the summit magmatic system, as well as within and around the summit vent. We begin by describing geodetic activity at Kīlauea's summit prior to 2008, changes to the magmatic system that this activity implied, and the network of instrumentation that monitored the 2008–2018 summit eruption, from its explosive onset on March 19, 2008, through 10 years of lava lake activity, to its conclusion coincident with the summit collapse and lower ERZ eruption of 2018 (Neal and others, 2019). We then examine the changes that occurred over the course of the eruption, first from a broad spatiotemporal perspective and then zeroing in on ever smaller (in magnitude) and shorter (in duration) signals that reflect a diversity of processes occurring in and around

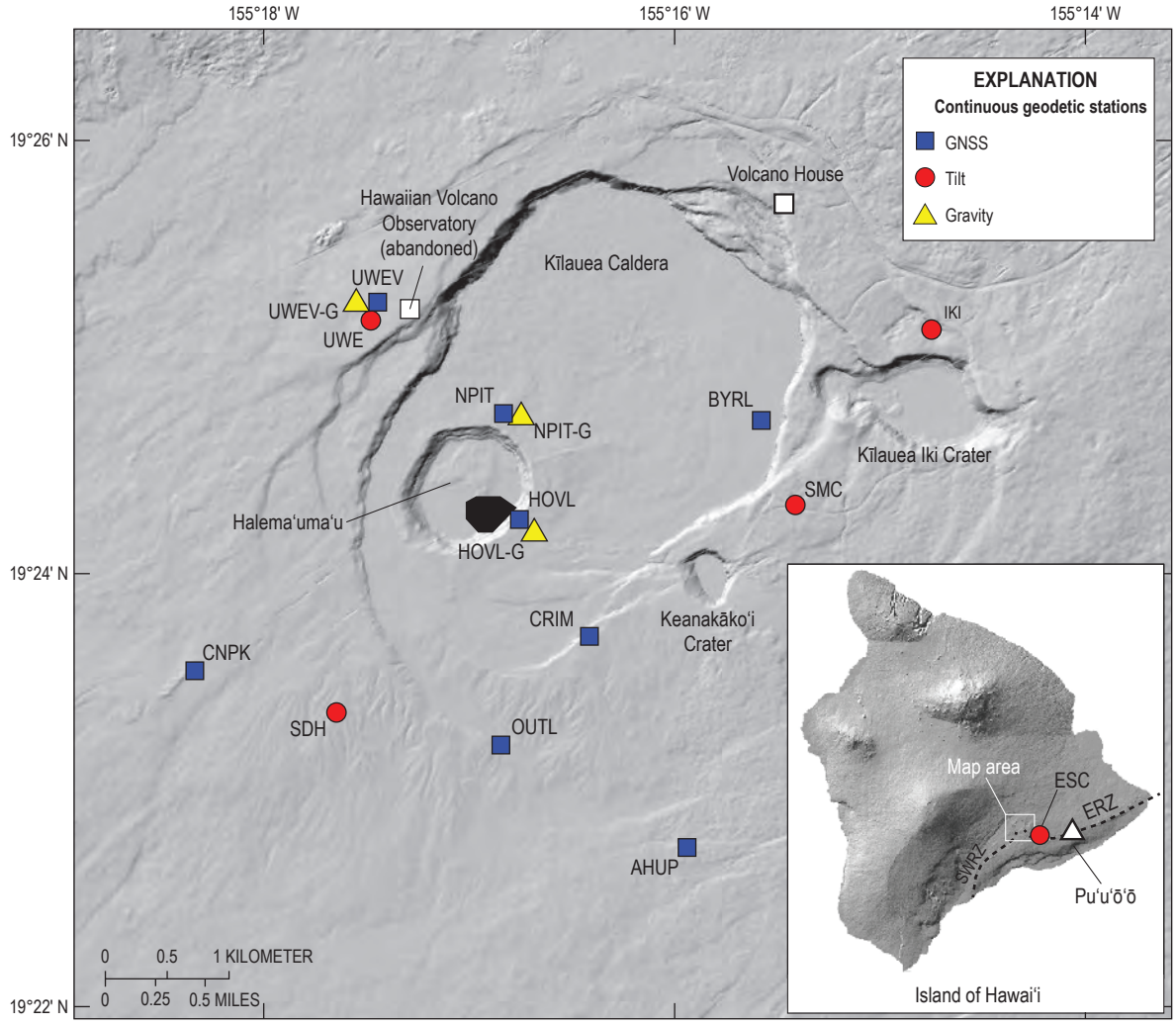


**Figure 1.** Map of continuous geodetic stations in Kīlauea's summit region (location of ESC tiltmeter is shown in the location map). Black polygon within Halema'uma'u indicates area occupied by the summit vent and persistent lava lake prior to the 2018 collapse. White squares show locations of the Hawaiian Volcano Observatory (abandoned after the 2018 collapse) and Volcano House hotel. Map area is given by white box in location map, which also shows the locations of the East Rift Zone (ERZ) and Southwest Rift Zone (SWRZ) (dashed lines) and Pu'u'ō'ō eruptive vent (white triangle). GNSS, Global Navigation Satellite System.

the summit vent and its underlying magmatic system. We conclude by pointing out open questions related to Kīlauea's 10-year-long summit eruption that geodetic data could play an important role in addressing.

## Deformation Monitoring at Kīlauea's Summit during 1912–2008 and Insights into the Volcano's Magmatic Plumbing System

Deformation measurements at the summit of Kīlauea began shortly after the establishment of the Hawaiian Volcano Observatory in 1912 (Tilling and others, 2014). Starting in 1913 and continuing through 1963, continuous ground tilt was documented by the wanderings of the recording line of a Bosch-Omori seismometer installed in the Whitney vault, near the present-day site of Volcano House on the northeast rim of Kīlauea Caldera (fig. 1; Jaggar and Finch, 1929; Decker and others, 2008; Wright and Klein, 2014). These continuous data were supplemented by occasional triangulation and leveling data, all of which revealed major changes in summit deformation over time—most notably related to the 1924 collapse of Halema'uma'u, located in the southwest sector of the caldera (Wilson, 1935; Wright and Klein, 2014). Jaggar and Finch (1929) also noted a correlation between lava-lake level and tilt, with rising lava level corresponding to tilt away from the summit caldera (similar to that observed during 2008–2018; Patrick and others, 2019b). These observations suggested the potential for eruption cycles, tidal forcing, and interactions with adjacent Mauna Loa, but such notions have since been

disproven (Patrick and others, 2019b). Nevertheless, the fundamental connection between lava level and ground deformation at Kīlauea's summit, as recognized early in the existence of the Hawaiian Volcano Observatory, holds true today.

This strategy of monitoring surface displacements using "seismometric" tilt and classical surveying techniques remained largely unchanged until the late 1950s, when water-tube tiltmeters were developed and deployed by Eaton (1959). These data were instrumental (pun intended) in quantifying major summit subsidence in 1960 and, with other data, for developing the first detailed magmatic model of Kīlauea (Eaton and Murata, 1960). The water-tube tiltmeter at Uēkahuna vault (collocated with site UWE in fig. 1) provided the longest continuous record of deformation for Kīlauea, and perhaps for any volcano, from 1956 to 2017 (fig. 2).

The 1960s were an important time for deformation monitoring at Kīlauea's summit, with leveling data showing rapid changes in the locus of uplift within the caldera between the 1965 ERZ eruption and 1967–1968 summit eruption (Fiske and Kinoshita, 1969). New techniques introduced during the decade were electronic distance measurement (EDM), to quantify changes in distance between survey points (Decker and others, 1966, 2008), and "spirit-level" or "dry" tilt measurements (Decker and others, 2008)—less accurate, but much less time consuming than water-tube measurements. The first "electronic" tilt monitoring began with the installation of a mercury-capacitance tiltmeter in the Uēkahuna vault in 1966 (Decker and others, 2008).

The next series of advances were in the late 1980s and 1990s, when most modern deformation monitoring stations and practices at Kīlauea were established. The period was dominated by the Puʻuʻōʻō eruption, which started in the middle ERZ (fig. 1) in 1983 and continued through a number of episodes until 2018 (Wolfe and others, 1988; Heliker and Mattox, 2003; Orr and others, 2015; Neal and others, 2019). Gravity measurements, first started in the 1970s (Dzurisin and others, 1980; Jachens and Eaton, 1980), became routine at Kīlauea's summit. Global Navigation Satellite System (GNSS) measurements (mostly utilizing Global Positioning System [GPS] technology), initially by campaign observations and then from continuously operating stations, supplanted EDM, and borehole tiltmeters began providing low noise, high sensitivity, and high temporal resolution records of deformation. By the early 2000s, interferometric synthetic aperture radar (InSAR) data from a growing constellation of satellites supplied high-spatial-resolution, line-of-sight displacement maps that were especially valuable for monitoring deformation of Kīlauea's unvegetated summit area (Decker and others, 2008).

These data, from 1913 onward, and the processes they tracked provided the basis for a refined magmatic model of Kīlauea's summit (fig. 3). The main magma storage area—the so-called south caldera reservoir—is located 3–5 kilometers (km) beneath the south part of the caldera and has long been recognized from persistent deformation in the area, especially subsidence prior to 2008 (for example, Dvorak and others, 1983; Davis, 1986; Yang and others, 1992; Cervelli and Miklius, 2003). The south caldera reservoir is generally recognized as being centered about 2 km south of the center of the caldera, although sometimes deformation associated with the source merges with that of the Southwest Rift Zone (fig. 1), leading to complex patterns of surface displacement. A second, smaller storage area—the so-called Halemaʻumaʻu reservoir—at 1–2 km depth below the eastern margin of pre-2018 Halemaʻumaʻu was initially proposed from models of transient tilt events in the early 2000s (Cervelli and Miklius, 2003) and confirmed by numerous subsequent studies (for example, Poland and others, 2009; Montgomery-Brown and others, 2010; Baker and Amelung, 2012; Lundgren and others, 2013; Anderson and others, 2015, 2019). Magma may also be stored near Keanakākoʻi Crater (fig. 1) at a few kilometers depth (Poland and others, 2014).

We envision the Halemaʻumaʻu and south caldera reservoirs to be connected, although the relation between the

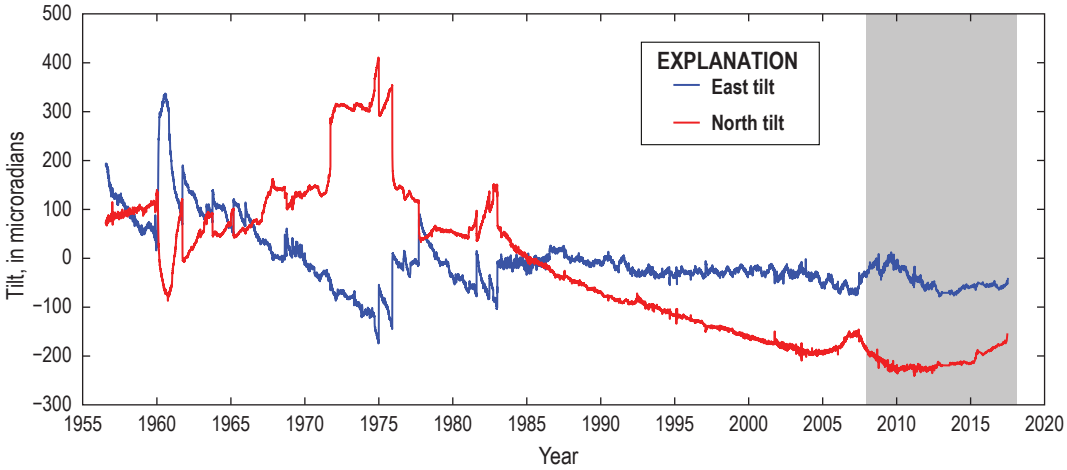


**Figure 2.** Plot of the water-tube tilt record from the Uēkahuna vault (collocated with site UWE in fig. 1). Because the tiltmeter is located mostly north of the deformation source near pre-2018 Halemaʻumaʻu, inflation and deflation of that source are strongly manifested as positive and negative tilt changes, respectively, in the north component. Gray area marks the 2008–2018 summit eruption.

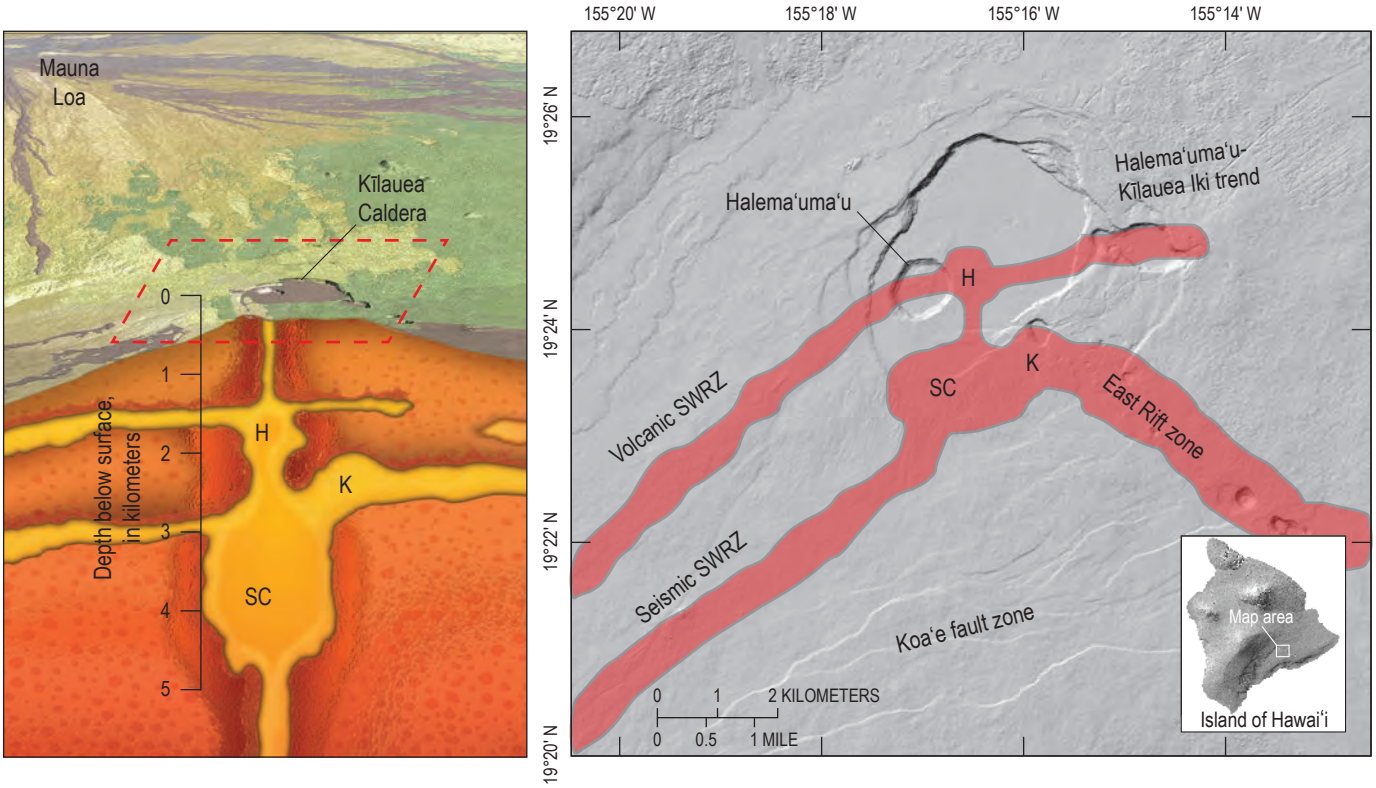


**Figure 3.** One possible schematic model of the magmatic plumbing system beneath the summit of Kīlauea. Left gives cross sectional view, right shows map view of the area outlined in red dashes and the locations of magma storage areas and conduits. H, Halema'uma'u reservoir; SC, south caldera reservoir; K, Keanakāko'i reservoir; SWRZ, Southwest Rift Zone. Adapted from Poland and others (2014).

two storage areas remains poorly understood (for example, Anderson and others, 2020; Wang and others, 2021; Wieser and others, 2021). Kīlauea's rift zones, which radiate east and southwest from the summit caldera, may be connected to the summit magmatic system via the south caldera reservoir at about 3 km depth; shallower conduits may also radiate from the Halema'uma'u reservoir—the so-called volcanic Southwest Rift Zone and Halema'uma'u- Kīlauea Iki trend (Poland and others, 2014). Together, the summit reservoirs and rift zones form an interconnected plumbing system through which magma is transported, as indicated by coincident changes in deformation signals since 1983 at the summit and 20 km away in the Pu'u'ō'ō area (Cervelli and Miklius, 2003; Anderson and others, 2015; Patrick and others, 2019a).

Throughout the 2008–2018 summit eruption, geodetic data and visual observations clearly established that the summit vent was connected to the Halema'uma'u reservoir, given the correlation between deformation attributed to that source and lava level changes within the vent (for example, Carbone and others, 2013; Anderson and others 2015). The summit vent was also connected hydraulically to eruptive vents at Pu'u'ō'ō and nearby based on the coincidence of deformation and lava level changes in both locations (Patrick and others, 2015, 2019a). Volume loss from the Halema'uma'u reservoir was the main cause of summit collapse during the 2018 lower ERZ eruption—the event that effectively terminated the 10-year-long summit eruption (Neal and others, 2019)—although only a portion of the reservoir was evacuated (Anderson and others, 2019).

## Geodetic Monitoring at Kīlauea's Summit, 2008–2018

At the start of Kīlauea's summit eruption, the network of continuously operating geodetic instrumentation included four borehole tiltmeters, one platform tiltmeter, and three continuous GNSS stations. Data from these sites (as well as infrequently used strainmeters; Anderson and others, 2015) were supplemented by InSAR observations, primarily from the ENVISAT and ALOS-1 satellites, and campaign gravity measurements across the caldera region that were repeated irregularly. Upon the onset of eruptive activity, however, the continuous GNSS network was expanded to eight stations, continuous gravity measurements were initiated at three sites within ~2 km of the vent, InSAR data became available from a growing constellation of satellites, and the frequency of gravity campaigns increased (fig. 4). Collectively, these data provided the coverage needed to detect, track, and interpret the varied geodetic behavior at Kīlauea's summit during 2008–2018.

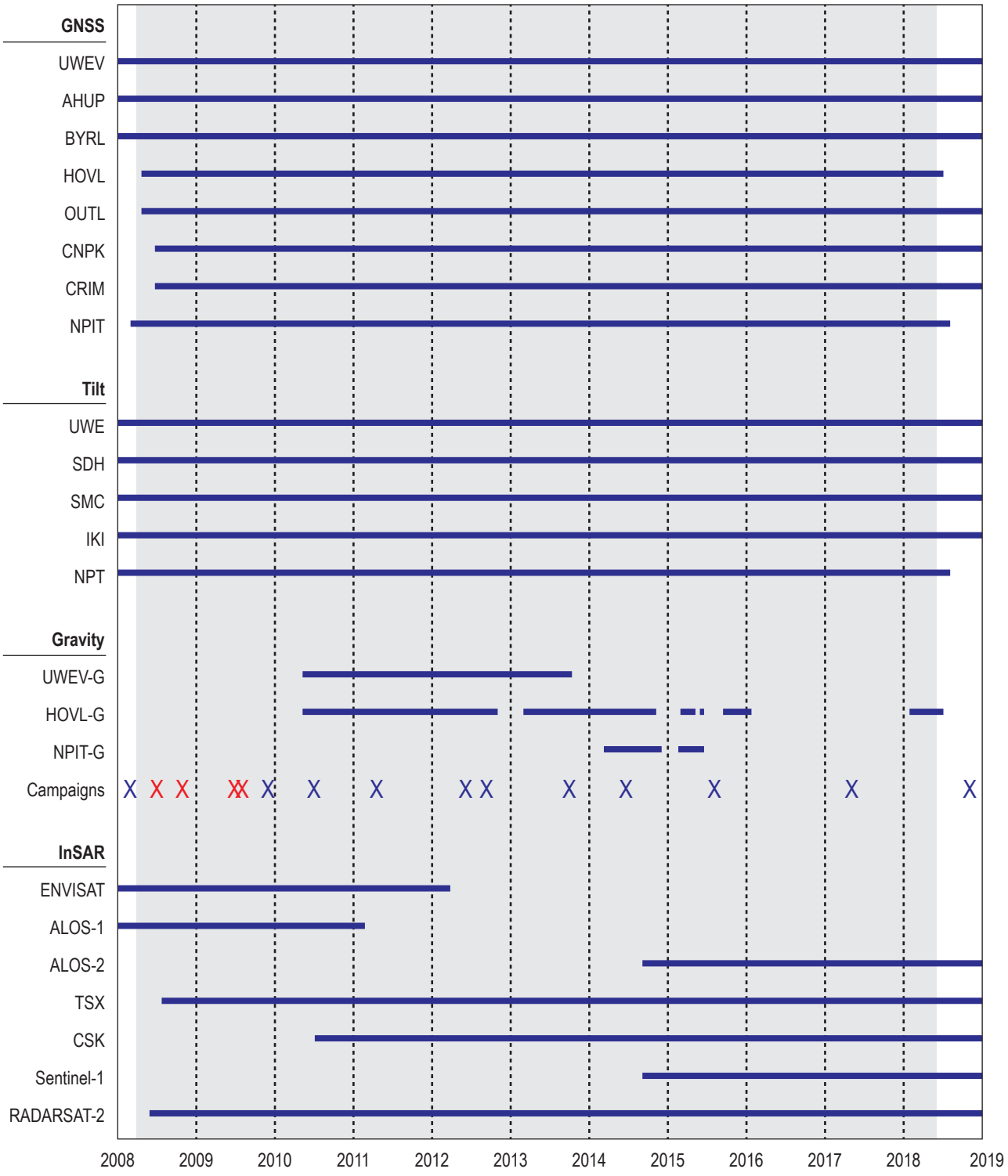


**Figure 4.** Graphical timeline of summit geodetic instrumentation and observations spanning 2008–2019. The period of the summit eruption is shaded gray. Campaign gravity measurements are noted by Xs, with red indicating surveys that were not useful owing to instrumentation problems. For site locations, see figure 1. GNSS, Global Navigation Satellite System; InSAR, interferometric synthetic aperture radar.

## Global Navigation Satellite System (GNSS)

At the start of 2008, the only continuous GNSS stations in operation in the summit area were UWEV, AHUP, and BYRL, and only the BYRL station was located within the main caldera (fig. 1). Station NPIT was installed just outside the North Pit vault on the northern edge of Halemaʻumaʻu on March 14 in response to an increase in gas emissions from the summit area (Sutton and Elias, 2014). In April 2008, after the March 19 eruption onset, stations HOVL and OUTL were established—the former on the east rim of Halemaʻumaʻu directly overlooking the eruptive vent. The network was rounded out by the installation of stations CRIM and CNPK in June. All stations were operational from the time they were established through the end of the summit eruption, but stations HOVL and NPIT were destroyed by the 2018 summit collapse (fig. 4). Near-annual GNSS campaigns were also conducted, including at a few sites in the summit region, but these data were not critical to interpretation of summit deformation, and campaign sites were largely replaced by continuous sites shortly after the onset of the 2008–2018 summit eruption.

## Tilt

The borehole tilt network remained unchanged throughout the summit eruption. Borehole tilt stations UWE, SDH, SMC, and IKI (figs. 3, 4) were in operation for several years before the eruption onset and functioned throughout the 10-year period of the eruption. Borehole UWE included two instruments, with a newer digital tiltmeter (designated UWD) installed on top of an older analog tiltmeter. The network was best suited to characterize transient deformation associated with the shallow Halemaʻumaʻu reservoir, although the UWE/UWD, SMC, and SDH instruments are approximately equidistant from the inferred source and, therefore, not well-suited for constraining its depth (Anderson and others, 2015). Diurnal signals at UWE were minimal, providing exceptional resolution of volcanogenic tilt at that site. Station IKI was far less sensitive to pressure changes within the Halemaʻumaʻu reservoir owing to its greater distance from that source, although major magmatic events were seen there, as well as at station ESC, which is in the upper part of the ERZ (fig. 1 inset). Station SMC consistently showed tilt azimuths indicating a source to the south of the Halemaʻumaʻu reservoir location, possibly owing to its proximity to the junction of the summit and ERZ magma systems (Anderson and others, 2015) and (or) topographic influences caused by the proximity of the caldera wall (Johnson and others, 2019).

A surface-mounted platform tiltmeter was located at the North Pit vault (close to GNSS station NPIT; fig. 1), but the data from this instrument were heavily affected by diurnal variations amounting to tens of microradians. The North Pit tiltmeter was never consistently used in deformation studies at Kīlauea.

## Gravity

A gravity survey was completed in the summit area in January 2008, 2 months prior to the onset of the summit eruption. Gravity change compared to previous surveys conducted in 1975, 1981, 1998, and 2003 suggested accumulation of 6–33 $\times 10^{10}$ kilograms (kg) (a volume of 21–120 $\times 10^{6}$ cubic meters [$m^3$] assuming a density of 2,800 kg/$m^3$) of magma in void space in the vicinity of the Halemaʻumaʻu reservoir, possibly contributing to the onset of eruption in 2008 (Johnson and others, 2010). Following the start of the summit eruption, gravity surveys were conducted episodically. Measurements later in 2008 and in early 2009 used a modified Lacoste and Romberg G-meter that did not function well, and these data are not useful. Starting in December 2009, however, surveys were performed using two Scintrex CG-5 instruments, resulting in higher data quality and robust measurements of gravity change (fig. 4; Bagnardi and others, 2014).

A new chapter in gravity monitoring was launched in 2010 with the establishment of continuously recording gravity stations at the summit of Kīlauea. These ultimately included a ZLS Burris gravimeter located in the Uēkahuna vault (2010–2013), a Lacoste and Romberg G-meter located at the Halemaʻumaʻu overlook (2010–2018), and a Lacoste and Romberg D-meter located near the North Pit vault (2014–2015) (figs. 3, 4; Poland and Carbone, 2016). All three instruments were collocated with GNSS stations (UWEV, HOVL, and NPIT, respectively) to allow for calculation of free-air effects.

## Interferometric Synthetic Aperture Radar (InSAR)

Early InSAR studies of Kīlauea included data acquisitions by the Shuttle Imaging Radar-C in 1994 (for example, Rosen and others, 1996) and occasional application of ERS-1/2 data to deformation events (Cervelli and others, 2002). The ERS-1/2 satellites did not have onboard recorders and there was no consistent and reliable downlink site in the region, so these data were not frequently exploited to study deformation of Hawaiian volcanoes. The JERS-1 satellite did have an onboard recorder but only acquired a handful of images of Kīlauea during the 1990s, although these were still useful for examining the 1993 ERZ intrusion (Conway and others, 2018). The situation improved dramatically in the late 1990s with the launch of RADARSAT-1, and in 2002 with the launch of the ENVISAT mission. Not only did both have on-board recorders, but they also featured a variety of imaging modes and look angles, allowing for frequent data acquisition—on average every 2–3 days—over Hawaiian volcanoes. ENVISAT could be tasked by scientific users, providing maximum flexibility for targeting of specific volcanic features.

ENVISAT experienced an orbit adjustment in 2010 and failed in 2012, but numerous additional InSAR-capable satellites were operational by that time, providing views of Kīlauea that spanned a range of wavelengths and ground

resolutions (fig. 4). The most frequently used of these systems included the X-band missions TerraSAR-X (2008–) and COSMO-SkyMed (2011–), the L-band missions ALOS-1 (2006–2011) and ALOS-2 (2014–), and the C-band missions Sentinel-1 (2014–) and RADARSAT-2 (2008–). Access to InSAR data was facilitated by the establishment of Hawai‘i as a supersite by the Group on Earth Observations in 2008—a status that was made permanent in 2012. Supersites were designated based on the existence of geologic hazards, the importance of the site for better understanding these hazards, the need for access to space-based data by local scientists and emergency managers for hazards assessment and preparedness, and the availability of ground-based data that could be freely shared among the research community (Salvi, 2016). Without the Hawaiian Volcanoes Supersite, both collection of, and access to, InSAR data over Kīlauea during 2008–2018 would have been severely limited.

## 10-Year Time Series

Based on continuous GNSS data, summit deformation during the 10 years of summit eruptive activity within Halema‘uma‘u can be separated into three phases: (1) from eruption onset to 2010, the summit subsided; (2) during 2010–2013 there was little net deformation, although several ERZ eruptive events, particularly in 2011, introduced summit inflation and deflation episodes over periods of weeks to months; and (3) from 2013 until the end of the summit eruption, variable levels of uplift and inflation occurred, interrupted occasionally by ERZ eruptive events and by a summit intrusion in mid-2015 (fig. 5).

Interferograms spanning both the entirety and subsets of the decade-long summit eruption emphasize the complex spatial patterns in surface displacements (fig. 6). GNSS and InSAR data suggest that the Halema‘uma‘u and south caldera reservoirs both contributed to the deformation field during 2008–2018. In interferograms spanning the summit eruption, the broadness of the summit deformation pattern and the density of fringes in the caldera (fig. 6) reflect the importance of the two magma storage zones to the overall deformation pattern. GNSS station AHUP is located southeast of the south caldera source and station HOVL is proximal to the Halema‘uma‘u reservoir (fig. 1), and over periods of months to years the two stations generally act in concert (fig. 5), indicating a coincidence in pressure change in the two reservoirs (short-term changes during summit and ERZ eruptive and intrusive activity, however, mostly reflected pressure change within the Halema‘uma‘u reservoir). One exception to this general long-term trend occurred from late 2011 to late 2012, when GNSS indicated uplift at station HOVL and slight subsidence at station AHUP (fig. 5)—a result corroborated by interferograms that clearly show inflation centered on the Halema‘uma‘u reservoir during that time (fig. 7).

The character of summit deformation during 2008–2018 was controlled largely by the balance between magma input from the mantle source and output from the Pu‘u‘ō‘ō vent

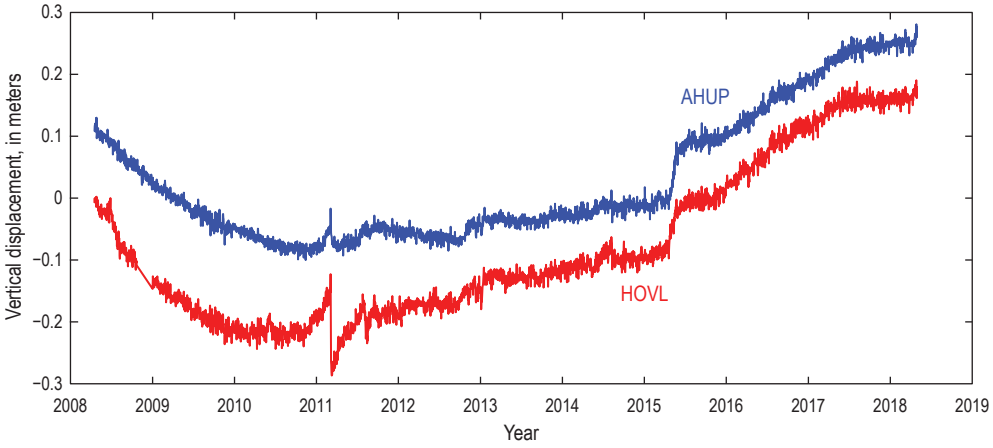


**Figure 5.** Plot showing vertical displacements at Global Navigation Satellite System (GNSS) stations AHUP (blue) and HOVL (red) spanning the 2008–2018 summit eruption. Both time series end on April 30, 2018, prior to the onset of major summit subsidence associated with the 2018 collapse. Station locations shown in figure 1. These stations were chosen because of their proximity to the Halema‘uma‘u (HOVL) and south caldera (AHUP) magma reservoirs. The stations track one another except from late 2011 through 2012, when AHUP shows subsidence and HOVL, uplift. Significant ERZ eruptive activity, like pre-, syn-, and post-event displacements associated with the March 5–9, 2011, Kamoamoa fissure eruption, is larger in amplitude at HOVL because the Halema‘uma‘u magma reservoir was more active than the south caldera reservoir during such events.

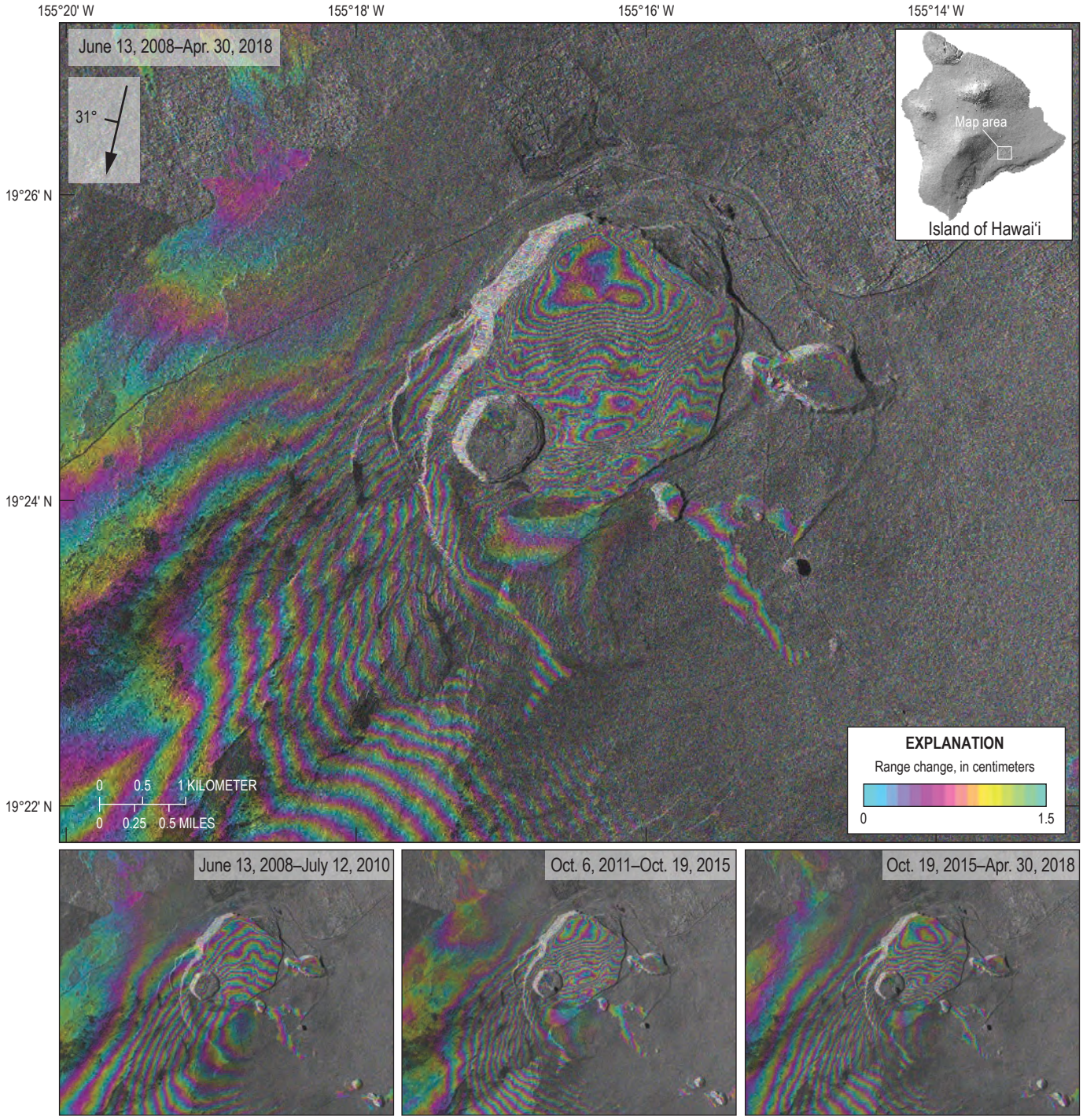


**Figure 6.** TerraSAR-X interferograms from descending track 24 (white box in location map shows area covered by the interferograms). Top image spans June 13, 2008–April 30, 2018 and shows line-of-sight displacements that occurred over the course of the 2008–2018 summit eruption. The complex nature of the fringe pattern reflects numerous short-term eruptive and intrusive events as well as long-term displacements. Motion of Kīlauea's south flank also contributes to the deformation field, but in the interferograms this effect is mostly south of the summit area. Concentric fringes in the north part of the caldera reflect persistent subsidence, perhaps related to a thick accumulation of cooling lava flows emplaced in the 19th and early 20th centuries. The three interferograms at the bottom span subsets of the 10-year period: June 13, 2008–July 12, 2010 (left); October 6, 2011–October 19, 2015 (middle), which includes the May 2015 summit intrusion; and October 19, 2015–April 30, 2018 (right). The period spanning late 2010 through late 2011 is omitted because displacements during that time were dominated by deformation associated with East Rift Zone eruptive events and related summit responses. In all periods, deformation is largely centered in the south part of the caldera, reflecting changes in magma storage within the south caldera reservoir.

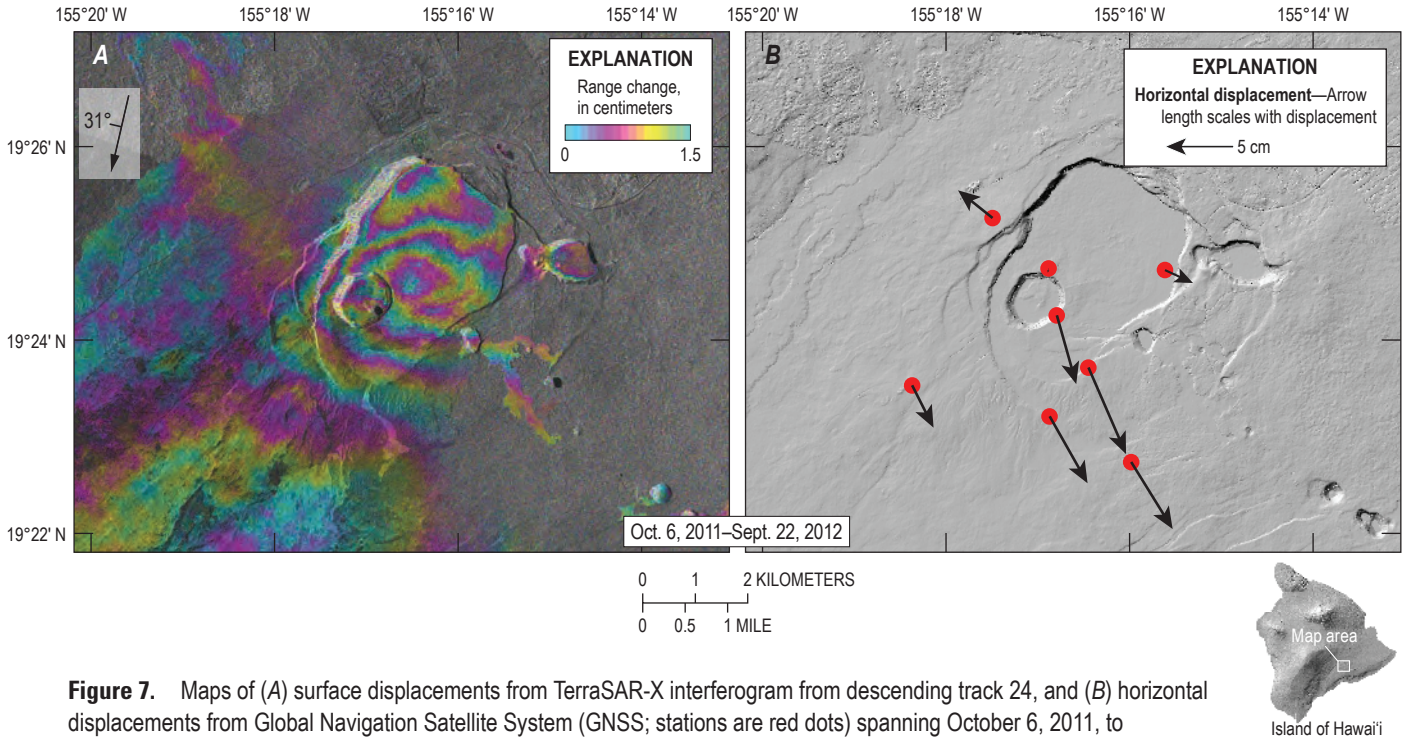


**Figure 7.** Maps of (*A*) surface displacements from TerraSAR-X interferogram from descending track 24, and (*B*) horizontal displacements from Global Navigation Satellite System (GNSS; stations are red dots) spanning October 6, 2011, to September 22, 2012. Confidence ellipses are omitted for clarity, but uncertainty is less than 1 centimeter (cm). White box in location map shows the area covered by both maps. Line-of-sight uplift in the interferogram is largely confined to the caldera (compare against interferograms shown in fig. 6) and GNSS vectors in the caldera area are largely radially away from the east margin of Halema'uma'u, reflecting magma accumulation in the Halema'uma'u magma reservoir. Slight line-of-sight subsidence in the interferogram is apparent in the south part of the caldera. GNSS and interferometric synthetic aperture radar (InSAR) results are consistent with the GNSS time series that indicate different motion in the central and south caldera areas during this period (fig. 5). Note that GNSS displacements in part *B* contain a component of south flank displacement, resulting in a few centimeters of southward motion.

on the ERZ. When input was greater than output, the summit inflated; deflation occurred when input was less than output. Changes in effusion rate at Pu'u'ō'ō created short-term (days to months) variations in summit deformation, but long-term trends over years appear to reflect changes in the rate of magma supply to the volcano, as well as the elevation of the ERZ eruptive vent (Patrick and others, 2019a). Based on geodetic, seismic, gas, and petrologic data, a doubling in magma supply occurred during 2003–2007 relative to previous years (Poland and others, 2012), after which time the volcano entered a magma supply lull, which lasted at least until 2012 (Poland, 2014; Anderson and Poland, 2016) and during which the volcano deflated or showed little net deformation (fig. 5). By 2016, magma supply had returned to pre-surge levels (Dzurisin and Poland, 2018), apparently outpacing the ERZ eruption rate given that the summit experienced persistent inflation after 2012 and until 2018 (fig. 5). This correlation reinforces the concept that magma supply exerts a strong control on the dynamics of Kīlauea.

An exceptional observation over the course of the summit eruption was the strong correlation between surface deformation and lava-lake level over time scales ranging from seconds to years (Patrick and others, 2015, 2019a,b; Poland and Carbone, 2016, 2018). The correspondence provided a rare window into pressure changes within a magma reservoir and led to important new insights into volcanic processes and physical properties, including the density of the lava lake (Carbone and others, 2013; Poland and Carbone, 2016, 2018; Poland and others, 2021), and the potential for anticipating changes in eruptive activity (Patrick and others, 2015). The lack of a temporal lag between surface displacements and lava level also suggests that, to a large degree, Kīlauea responded elastically to reservoir pressure changes. Perhaps most notably, the pressure changes indicated by joint analysis of lava level and surface deformation facilitated quantitative estimates of the volume of the Halema'uma'u magma reservoir (Anderson and others, 2015, 2019)—a result that would not have otherwise been possible. The use of lava level as a gauge for magma reservoir pressure is thus one of the most noteworthy advances resulting from geodetic and other data collected during Kīlauea's decade-long summit eruption.

Unlike the variations in surface deformation, gravity in the vicinity of Halema'uma'u showed persistent increases

over the course of the summit eruption based on campaign measurements. A gravity survey completed just prior to the onset of the summit eruption in 2008 suggested a significant mass increase within the Halemaʻumaʻu reservoir since 1975, despite the lack of corresponding surface uplift. Johnson and others (2010) interpreted this apparent contradiction to indicate magma accumulation in void space—probably in the form of a network of interconnected cracks and open spaces in the vicinity of the Halemaʻumaʻu magma reservoir—as the system recharged prior to the onset of the summit eruption. Mass increase in the Halemaʻumaʻu reservoir persisted following the onset of eruption. Continued filling of void space might account for this increase, but Bagnardi and others (2014) proposed that it could also indicate subtle densification (by less than 200 kg/m$^3$) of subsurface magma owing to degassing via the summit vent.

Continuous gravity monitoring was in place for much of the summit eruption at station HOVL-G and for a few years also at station UWEV-G (figs. 1, 4). Joint analysis of the data from these stations in 2010 suggested rapid convection in the Halemaʻumaʻu magma reservoir—an insight that would not be possible to determine from any other dataset (Carbone and Poland, 2012). For the bulk of the eruption, however, only the HOVL-G continuous gravity station was operational. Although not useful for assessing long-term subsurface mass changes because of instrument drift, short-term measurements over days to weeks were still useful for assessing the density of the upper tens to hundreds of meters of the summit lava lake. Continuous data collected between 2011 and 2015 indicate a lava lake density of 1,000–1,500 kg/m$^3$, and that the density may have increased slightly over that time period or that the vent enlarged over time to hold a greater mass of magma (Poland and Carbone, 2016).

Changes in deformation style at Kīlauea's summit over the course of the 2008–2018 eruption occurred gradually, evolving from deflation to inflation, probably reflecting patterns of magma supply. The period was, however, punctuated by several transient deformation events. These most frequently were related to the formation of new eruptive vents at or near Puʻuʻōʻō (Patrick and others, 2015, 2019a), but at least one instance was unambiguously a result of a summit intrusion.

# Major Summit Transient Deformation Events

Changes in deformation sense and style at Kīlauea's summit can be a result of magmatic intrusions and eruptions not only in the summit area, but also along the volcano's rift zones. The 1924 summit collapse resulted from an intrusion into the lower ERZ (Wright and Klein, 2014), subsidence in 1960 was associated with magma withdrawal from the summit to feed the Kapoho eruption in the lower ERZ (Eaton and Murata, 1960; Wright and Klein, 2014), and the 2018 lower ERZ eruption resulted in summit collapse (Neal and others, 2019). Smaller scale subsidence and deflation at the summit occurs in response to smaller rift zone eruptions and intrusions, for example, those of 1993 (Conway and others, 2018), 1997 (Owen and others, 2000), 1999 (Cervelli and others, 2002), and 2007 (Poland and others, 2008; Montgomery-Brown and others, 2010). Intrusions beneath the summit region were common in the 1960s and 1970s (for example, Fiske and Kinoshita, 1969; Dvorak and others, 1983; Yang and others, 1992) but only one, in 2015, was well documented after the onset of the Puʻuʻōʻō eruption in 1983.

## ERZ Source: The 2011 Kamoamoa Eruption and Subsequent Activity

Several times throughout the 2008–2018 summit eruption, accumulation of magma in the ERZ owing to waning lava effusion, presumably from a breakdown of conduit systems near the ERZ eruptive vent, caused summit inflation and eventually culminated in the formation of a new eruption site on or near Puʻuʻōʻō (Patrick and others, 2019a). These magmatic sources were superimposed on long-term motion of Kīlauea's south flank, which caused extension across the ERZ and effectively primed parts of the rift for intrusions at quasi-regular intervals (Montgomery-Brown and Miklius, 2021). The most significant such sequence occurred in 2011, starting with the Kamoamoa fissure eruption in March and repeating twice more that year.

The first indication of the impending Kamoamoa eruption manifested in late 2010—waning rates of lava effusion from Puʻuʻōʻō were associated with summit uplift and seismicity as Kīlauea's magmatic system, from the ERZ to the summit, began to pressurize (Orr and others, 2015). Resulting summit inflation was centered on the east margin of Halemaʻumaʻu, indicating pressure increase within the Halemaʻumaʻu reservoir (fig. 8*A*). Summit uplift reached about 7 cm between late 2010 and March 2011 at GNSS station HOVL. On March 5, 2011, the magmatic system ruptured and the Kamoamoa fissure eruption began about 2 km uprift of Puʻuʻōʻō.

The Kamoamoa eruption was accompanied by rapid subsidence of the summit as magma drained to feed the ERZ fissure (fig. 9). As was typical of ERZ intrusions and eruptions during the 1983–2018 Puʻuʻōʻō activity, deflationary summit tilt decayed quasi-exponentially, flattening after about 2 days; inflationary tilt began immediately upon cessation of the Kamoamoa eruption on March 9 (fig. 10). Models of interferograms spanning the eruption (fig. 8*B*) indicated a volume loss of $1.7\times10^6$ m$^3$ at a depth of 1.7 km—the location of the Halemaʻumaʻu magma reservoir (Lundgren and others, 2013). The same reservoir began pressurizing after the eruption's end (fig. 8*C*). This pattern—gradual inflation, rapid exponentially decaying deflation, and gradual reinflation—repeated twice more in 2011 (fig. 9), during a breakout from the side of the Puʻuʻōʻō cone that resulted in a rapidly emplaced lava flow in August, and in response to the formation of a new long-term eruptive vent on the flank of Puʻuʻōʻō in late September.

One of the more unique insights resulting from the Kamoamoa eruption was the calculation of summit lava-lake

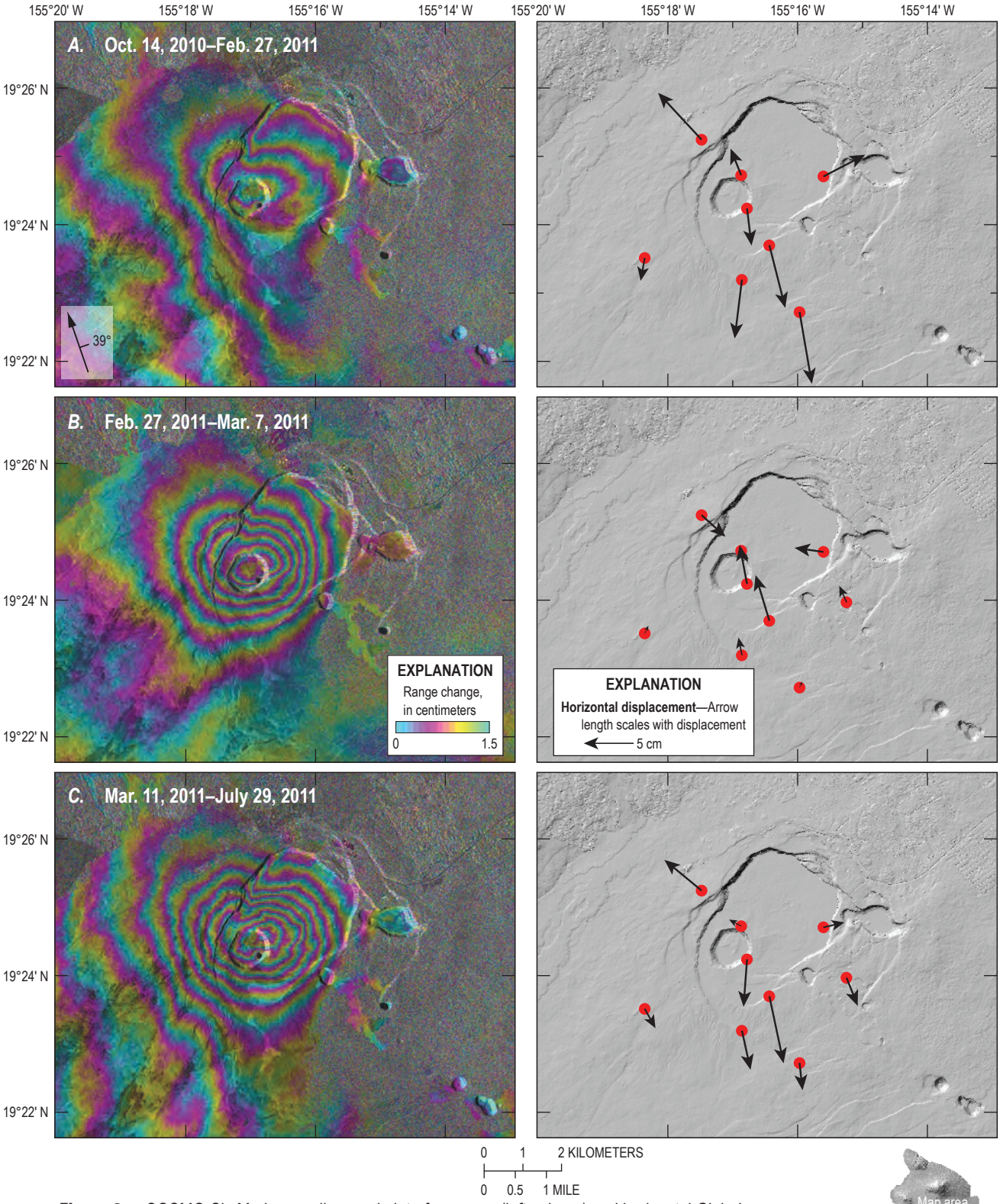


**Figure 8.** COSMO-SkyMed ascending-mode interferograms (left column) and horizontal Global Navigation Satellite System (GNSS) displacements (right column) spanning periods before (*A*), during (*B*), and after (*C*) the Kamoamoa fissure eruption on Kīlauea's East Rift Zone. The pre-event period was characterized by summit inflation, which reversed during the event itself. Following the end of the eruption, the summit reinflated (fig. 9). All episodes of deformation were centered on the Halema'uma'u magma reservoir. Confidence ellipses are omitted in the horizontal GNSS dispacement maps, but uncertainty is less than 1 centimeter.

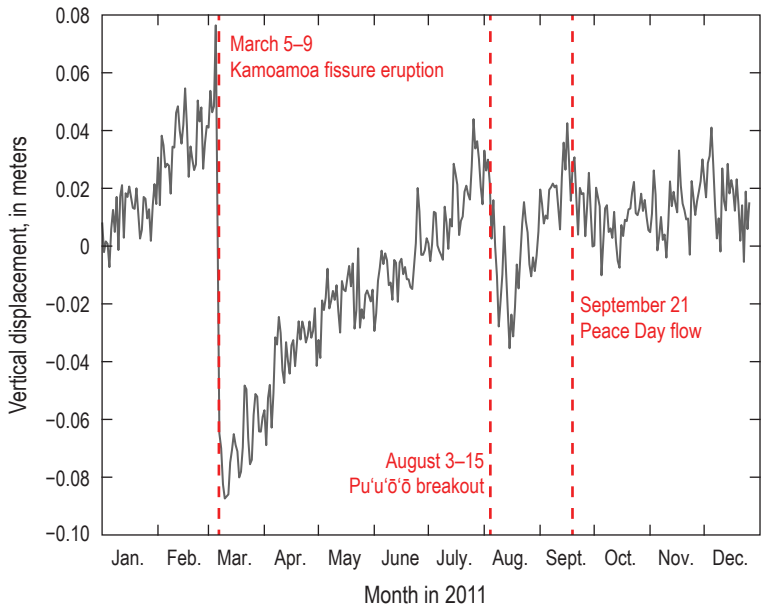


**Figure 9.** Plot of vertical displacements at Global Navigation Satellite System (GNSS) station HOVL (fig. 1) during 2011. Eruptive events on the East Rift Zone, which led to an increase in the rate of magma withdrawal from, and subsidence of, the summit, are noted by dashed red lines.

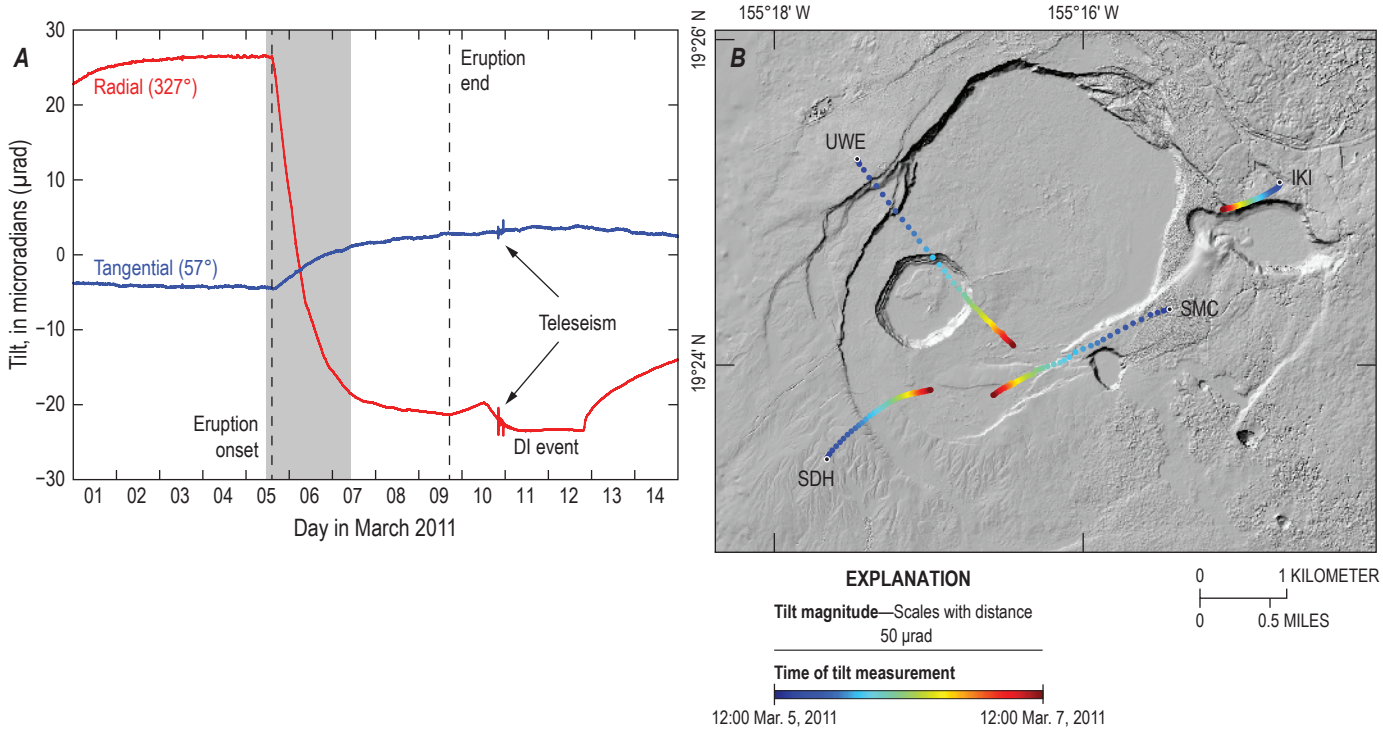


**Figure 10.** Plot and map showing tilt measurements during the Kamoamoa fissure eruption. *A*, Tilt measured by continuous borehole instrument UWE (location in fig. 1) spanning the March 5–9, 2011, Kamoamoa fissure eruption. The radial component is oriented toward the main summit deformation source beneath the east rim of Halema'uma'u, and the tangential component is orthogonal to that direction. Tilt azimuths are given in degrees. Eruption start and end times are noted by dashed black lines. Gray bar indicates time spanned by data in part *B*. Summit inflation commenced immediately upon the end of the eruption. A deflation-inflation (DI) event interrupted the reinflation shortly after its onset. Increased noise late on March 10 is associated with the arrival of teleseisms associated with the magnitude-9 Tohoku, Japan, earthquake. *B*, Map showing the progression of tilt direction at summit stations between 12:00 p.m. Hawaii Standard Time (HST) on March 5, 2011, and 12:00 p.m. HST on March 7, 2011. Colors correspond to time, and the length of trails indicates tilt magnitude. Sampling rate (dot spacing) is 60 minutes.

density using combined gravity, deformation, and lava level data. The continuous gravimeter at station HOVL-G recorded a gravity decrease of about 150 microgals (μGal) in the first 14 hours of the activity, with the lava-lake level receding by 120 meters (m) and the ground subsiding by about 15 cm (Carbone and others, 2013). Thanks to detailed knowledge of the summit-vent geometry, Carbone and others (2013) were able to model the temporal progression of the gravity decrease and lava-lake withdrawal by assuming a lava-lake density of 950±300 kg/m$^3$, indicating that the upper 120 m of the lava lake was rich in gas. This density is consistent with that obtained from measurements over the entirety of 2011–2015 (Poland and Carbone, 2016) and is information that could not have been obtained using any other dataset.

## Summit Source: The 2015 Intrusion

Throughout the 1960s, 1970s, and early 1980s, intrusions and eruptions were common in the summit region of Kīlauea. These were mostly documented by leveling, EDM, and water-tube tilt measurements, from which modeling established that subsidence sources were mostly located in the south part of the caldera, whereas inflation sources were spatially more scattered (for example, Fiske and Kinoshita, 1969; Dvorak and others, 1983; Davis, 1986; Yang and others, 1992). Intrusions and eruptions at the summit stopped, however, in 1983, with the onset of the Pu‘u‘ō‘ō eruption on the ERZ. Thus, no summit intrusions had been documented with modern geodetic monitoring—like GNSS, InSAR, and borehole tilt—for many subsequent years.

It was therefore something of a surprise when a summit intrusion occurred in May 2015. The intrusion was preceded by weeks of summit inflation, which began suddenly on about April 21 (figs. 11, 12*A*), and rising lava-lake levels that increased to the point of overflowing onto the floor of Halema‘uma‘u for the first time since the beginning of the summit eruption in 2008 (Patrick and others, 2019a,b, 2021; Bemelmans and others, 2021). The lava-lake height increase and pattern of deformation indicated pressurization of the Halema‘uma‘u reservoir (Bemelmans and others, 2021). Summit inflation plateaued in late April and early May, and on May 11 the summit began to deflate suddenly (figs. 11, 12*B*) and the lava level started to fall, again because of pressure changes within the Halema‘uma‘u reservoir (Bemelmans and others, 2021). On May 12, a change in the tilt direction indicated a new phase of activity, which, when combined with

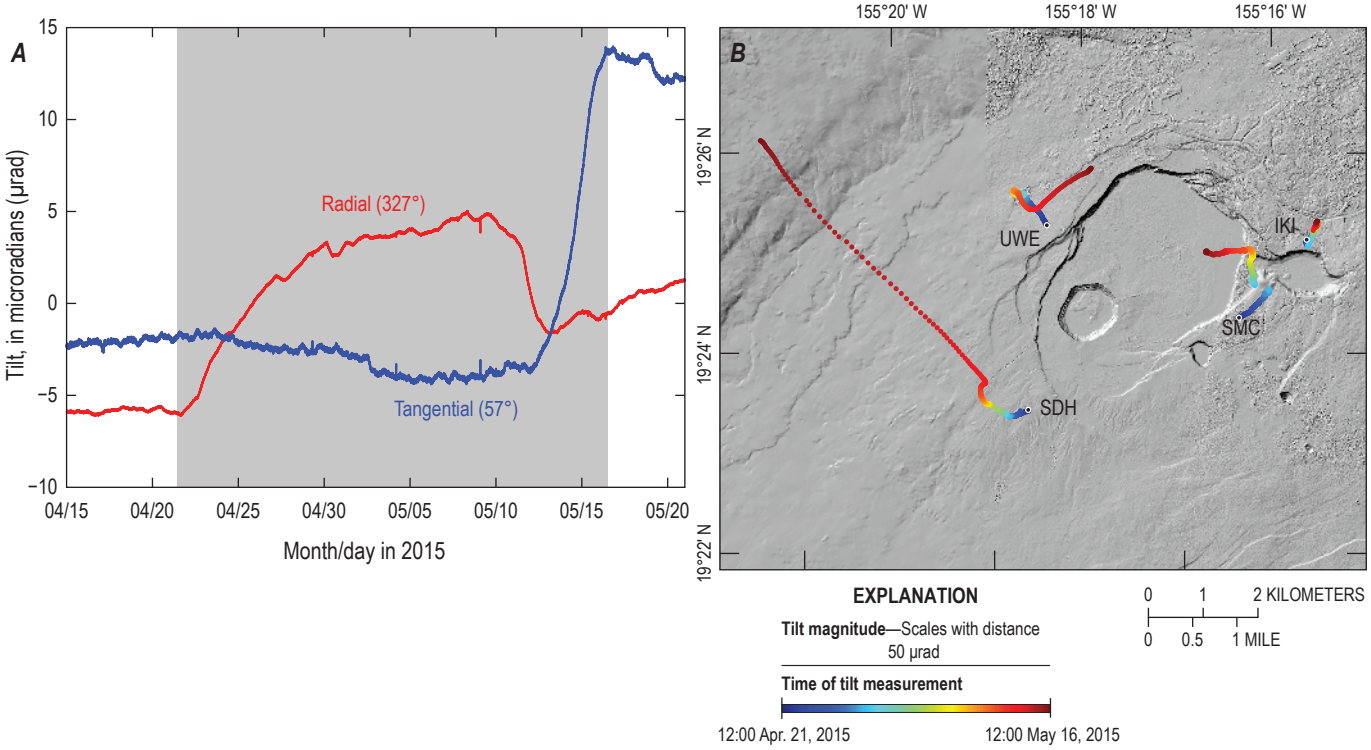


**Figure 11.** Plot and map showing tilt measurements during the 2015 summit intrusion. *A*, Tilt measured by continuous borehole instrument UWE (location in fig. 1) spanning April 15–May 20, 2015, which includes the mid-May summit intrusion. The radial component is oriented toward the main summit deformation source, and the tangential component is orthogonal to that direction. Tilt azimuths are given in degrees. Gray bar indicates time spanned by data in part *B*. Inflation (positive radial) deformation began in late April and was coincident with a rise in the level of the summit lava lake. Deflation began on May 11 along with lava-level drop, and on May 12 a rapid change in the tangential tilt component indicated the onset of an intrusion in the south part of the caldera. *B*, Map showing the progression of tilt at summit stations between 12:00 p.m. Hawaii Standard Time (HST) on April 21, 2015, and 12:00 p.m. HST on May 16, 2015. Colors correspond to time, and the length of trails indicates tilt magnitude. Sampling rate (dot spacing) is 60 minutes.

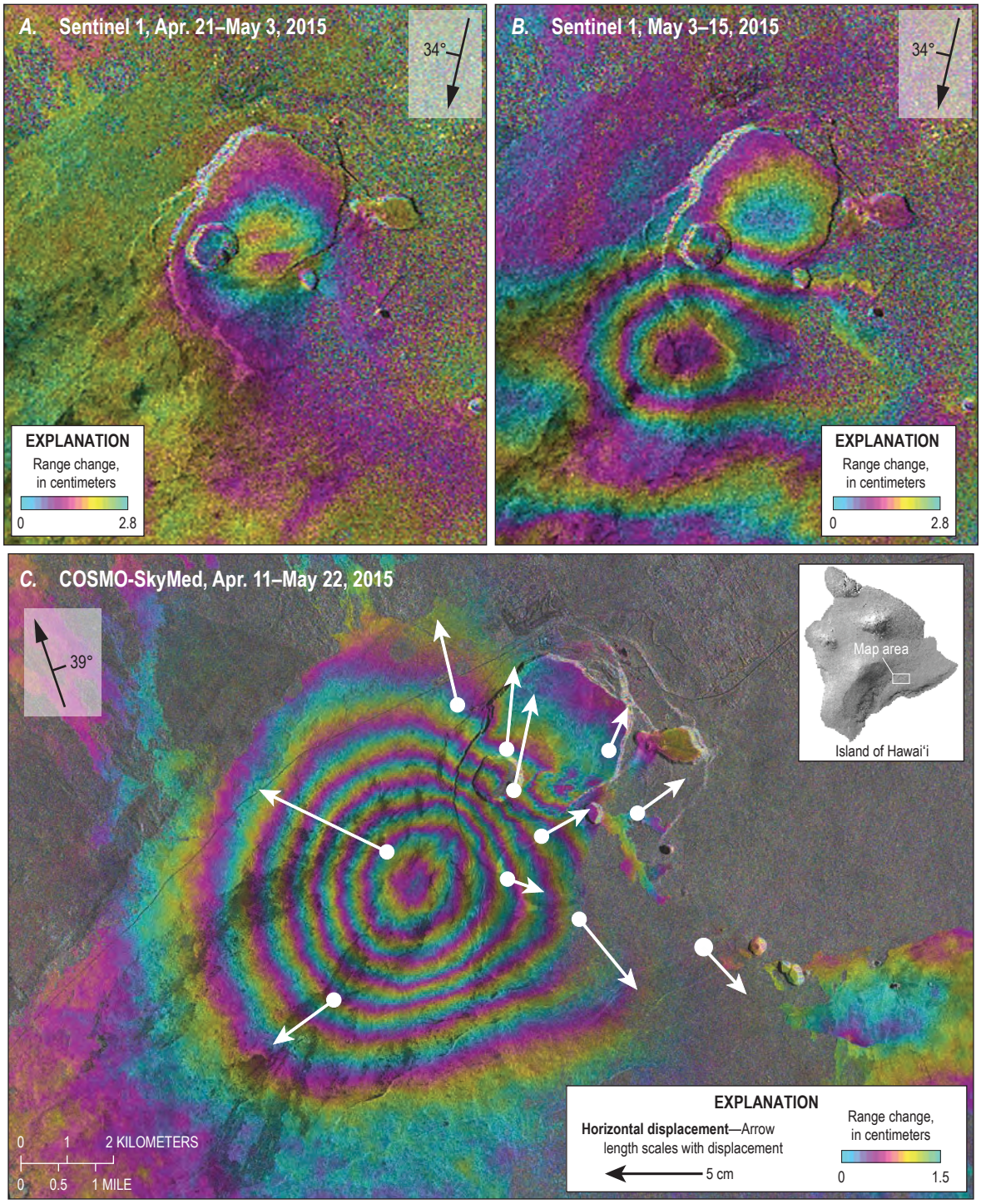


**Figure 12.** Interferograms showing deformation of Kīlauea's summit during the 2015 intrusion. *A*, Sentinel-1 descending interferogram spanning April 21–May 3, 2015, showing line-of-sight uplift in the center of the caldera owing to pressurization of the Halema'uma'u magma reservoir. *B*, Sentinel-1 descending interferogram spanning May 3–15, 2015, with line-of-sight subsidence in the caldera center and uplift in the south part of the caldera, indicating depressurization and pressurization of the Halema'uma'u and south caldera magma reservoirs, respectively. C, COSMO-SkyMed ascending interferogram and Global Navigation Satellite System (GNSS) horizontal displacements spanning April 11–May 22, 2015, illustrating the overall deformation field associated with the May 2015 summit intrusion, which is dominated by south caldera line-of-sight uplift. Confidence ellipses for the horizontal displacements are omitted for clarity, but uncertainty is less than 1 centimeter. Location map in part *C* shows the area covered by that interferogram; parts *A* and *B* cover slightly smaller areas.

the progression of shallow seismicity, indicated an intrusion in the south part of the caldera—an interpretation corroborated by InSAR (fig. 12*B*,*C*). Jo and others (2015) and Bemelmans and others (2021) modeled COSMO-SkyMed and Sentinel interferograms, respectively, and found a source depth of about 3 km beneath the south caldera—approximately coincident with the south caldera magma reservoir and consistent with the emplacement of a stock or similar structure on the margin of that body.

Intriguingly, the south caldera intrusion was not manifested in deformation data until after the shallower Halemaʻumaʻu reservoir had been draining for about a day, suggesting that the magma input from this source was necessary to propagate the intrusion, or that the pathway between the two sources was temporarily blocked—this despite the interpretation that the intrusion must have already initiated to cause the magma drainage from the summit eruptive vent. This forms the basis for a perplexing chicken-or-egg problem but argues for connectivity between the Halemaʻumaʻu and south caldera magma reservoirs (Bemelmans and others, 2021)—an interpretation that has been cited as ambiguous (Anderson and others, 2020; Wang and others 2021).

The 2015 intrusion may be similar to intrusions that occurred in the 1960s and 1970s, with the south caldera magma reservoir serving as the initiation point. This explains why inflation sources during that time period were spatially diverse—because intrusions might initiate from anywhere on or around the south caldera reservoir. The event also raises the possibility that some summit eruptions originate from the south caldera reservoir, rather than through the shallower Halemaʻumaʻu reservoir—a possibility that might explain the higher MgO content of some lava flows on the caldera margins (Helz and others, 2014). Data from 2015 do not yet, however, indicate a driving mechanism for the intrusion, nor the reason it initiated from the south caldera instead of the shallower Halemaʻumaʻu reservoir. Bemelmans and others (2021) suggest that a short-term increase in magma supply caused the intrusion but cannot rule out other factors, like filling of void space and changes in the efficiency of magma transport along the ERZ.

# Minor Summit Transient Deformation Events

Substantial transient summit deformation events of the 2008–2018 eruption received significant scientific and public attention because of their association with summit and ERZ intrusions and eruptions, but minor transient events also occurred. Some of these were nearly continuous, like so-called deflation-inflation (DI) events, whereas others were occasional and ambiguous in character and origin, possibly representing small intrusions, or were spatially localized, especially around the summit eruptive vent.

## Deflation-Inflation (DI) Events

Deflation-inflation (DI) events were first identified in 2000, shortly after the installation of borehole tiltmeters at the summit of Kīlauea in 1998 (Cervelli and Miklius, 2003). The events were commonly associated with changes in lava effusion from ERZ eruptive vents, with waning effusion during the deflation phase and increased effusion during inflation phases, albeit with a lag of tens of minutes to a few hours compared to the onsets of these phases at the summit (Cervelli and Miklius, 2003; Anderson and others, 2015). DI events were almost certainly occurring prior to 1998 as well, given minor deflation and inflation patterns recorded on a mercury-capacitance tiltmeter at Kīlauea's summit and coincident observations of changing effusion rate from the ERZ eruptive vents (Anderson and others, 2015); these were referred to as "surge" events by Heliker and Mattox (2003). Models of DI events indicate that the deformation source centroid is located 1–2 km beneath the eastern margin of the former Halemaʻumaʻu crater, which is the region of the Halemaʻumaʻu magma reservoir (Poland and others, 2014; Anderson and others, 2015).

Prior to the onset of the summit eruption in 2008, DI events were infrequent, with typically a few per year. Following the eruption onset, however, the rate of DI event occurrence increased substantially, and some years had more than 100 events. Ground deformation was strongly correlated with lava level in the summit eruptive vent, with decreases in lake-surface height during deflation and increases during inflation—the largest DI events were associated with changes in lava level as great as 50 m (Anderson and others, 2015). Coupled deformation and lava-level observations provided an opportunity to model the volume of magma storage in the Halemaʻumaʻu reservoir, estimated to be 0.2 to 5.5 cubic kilometers ($km^3$) (at 95 percent confidence level) by Anderson and others (2015). Later modeling by Anderson and others (2019) using data recorded as the magma system drained in the early part of the 2018 eruption indicated a somewhat larger volume.

That the occurrence rate of DI events increased markedly with the onset of the summit eruption in 2008 suggests a causal relationship. Notably, $SO_2$ gas flux increased by several times with the opening of the summit vent and remained high for the duration of the eruption (Sutton and Elias, 2014). One hypothesis is that DI events were related to convective overturns in the shallow summit magma reservoir (fig. 13). In this conceptual model, convective overturn of degassing magma within the Halemaʻumaʻu reservoir and downward flow from that storage area impedes recharge of the reservoir and flow of magma to the ERZ. Then, within hours to a few days, gas-rich magma ascends again into the reservoir, causing reinflation and a rise in the lava-lake level at the summit, and reinvigorating magma transport with the ERZ conduit. This model, however, cannot explain large variations in the rate of

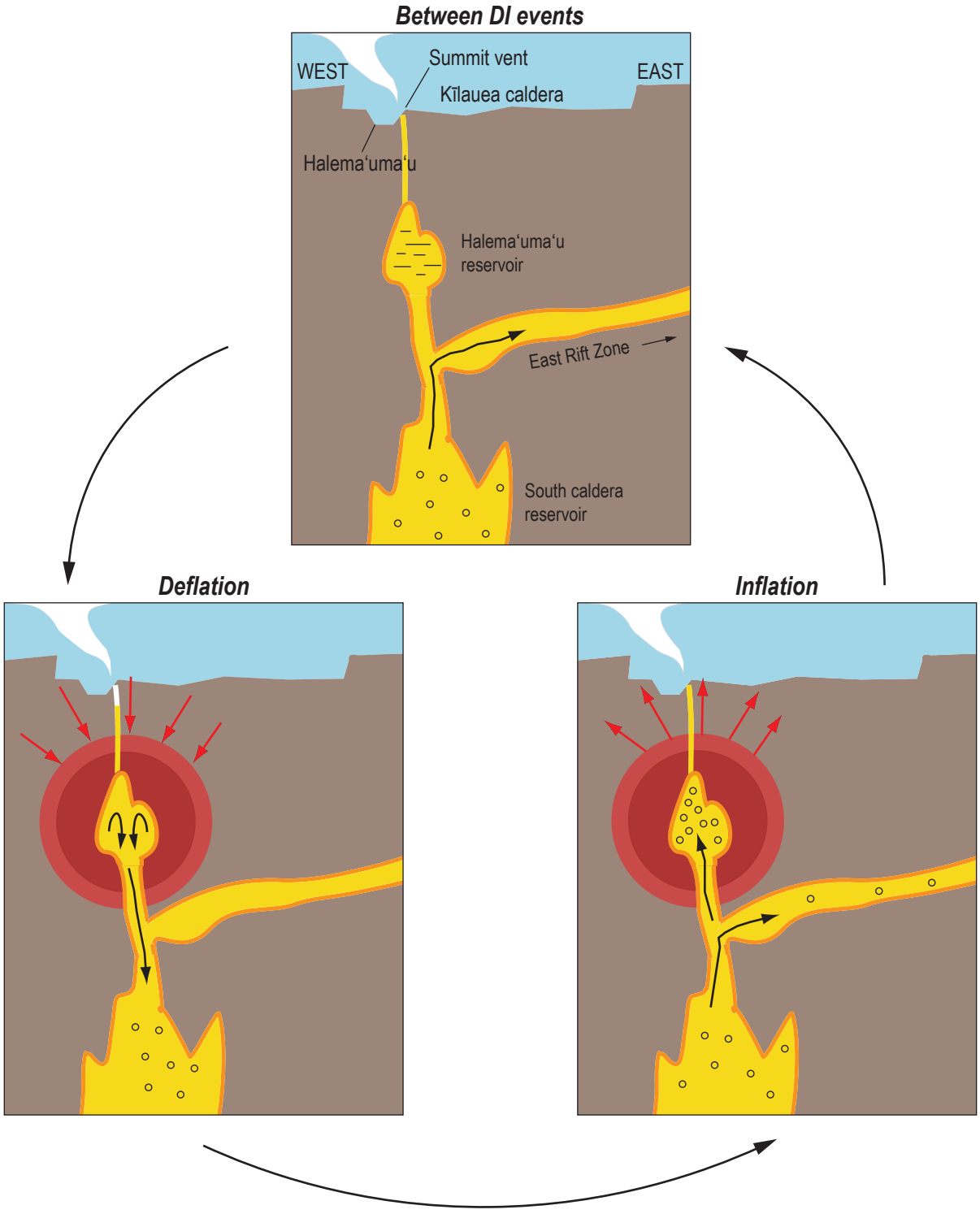


**Figure 13.** Schematic east-west cross section across Kīlauea Caldera illustrating a conceptual model for cyclic deflation-inflation (DI) events. Note that the relation between the Halema'uma'u reservoir, the south caldera reservoir, and the outlet(s) to the East Rift Zone (ERZ) are not well known (see "What is the Geometry of Summit Magma Storage?" section). During the inter-event period, magma continuously degasses from the Halema'uma'u reservoir and the overlying conduit. As it degasses, the magma becomes denser and a convective overturn occurs, resulting in a pressure decrease and deflation of the Halema'uma'u reservoir. Sinking denser magma interrupts magma flow to the ERZ. Gas-rich magma from depth eventually overcomes the blockage and rises back into the Halema'uma'u reservoir, causing pressurization, inflation, and reestablishment of magma flow to the ERZ. Although it is consistent with many aspects of DI events, this model fails to explain some observations, such as the irregular rate of DI events and their continued occurrence after the 2018 summit collapse and partial draining of the Halema'uma'u reservoir. Other unknown mechanisms probably also play a role.

DI event occurrence over time (Anderson and others, 2015). Open questions also remain about the possible accumulation of magma in the south caldera reservoir during the deflation phase of an event—a process that has not been detected geodetically (Anderson and others, 2020). The mechanism of DI events and their importance remains ambiguous, but their increased rate of occurrence during the summit eruption and persistence during post-2018 collapse recharge would seem to provide key evidence to their origin.

## Small Intrusions

The May 2015 summit intrusion was unmistakable because of the accompanying seismicity and deformation. Evidence from both seismic and geodetic data during 2008–2018 indicates the possibility of multiple smaller summit intrusions as well. These intrusions may have involved injections of magma into cold host rock or into warm, mushy, crystal-rich areas of existing reservoirs. Similar events may have gone unnoticed prior to the 2008 densification and upgrading of summit-monitoring networks.

One possible small intrusion occurred in late October 2012 and was most clearly reflected in borehole tilt data (fig. 14). After a DI event on October 26–27, the summit started to deflate on October 28, but the tilt pattern (particularly at station SMC) did not resemble that of most DI events, even though the deflation magnitude was similar. At the same time, seismicity in the area of Keanakāko‘i Crater increased. These data indicated a potential small intrusion in that area, although InSAR showed no anomalous surface deformation there, probably owing to the combination of poor coherence and the small magnitude of any signal. A leveling survey was conducted in the area on October 31, 2012, and results were compared to those from a previous survey in February 2011. The leveling data showed approximately 1 cm of uplift in excess of that expected from summit inflation near Keanakāko‘i Crater (fig. 15), consistent with the possibility of a small intrusion. This event occurred at the end of a period of accelerated uplift in the broader summit region (fig. 14), suggesting that rapid pressurization might have led to a small rupture of the summit magma system.

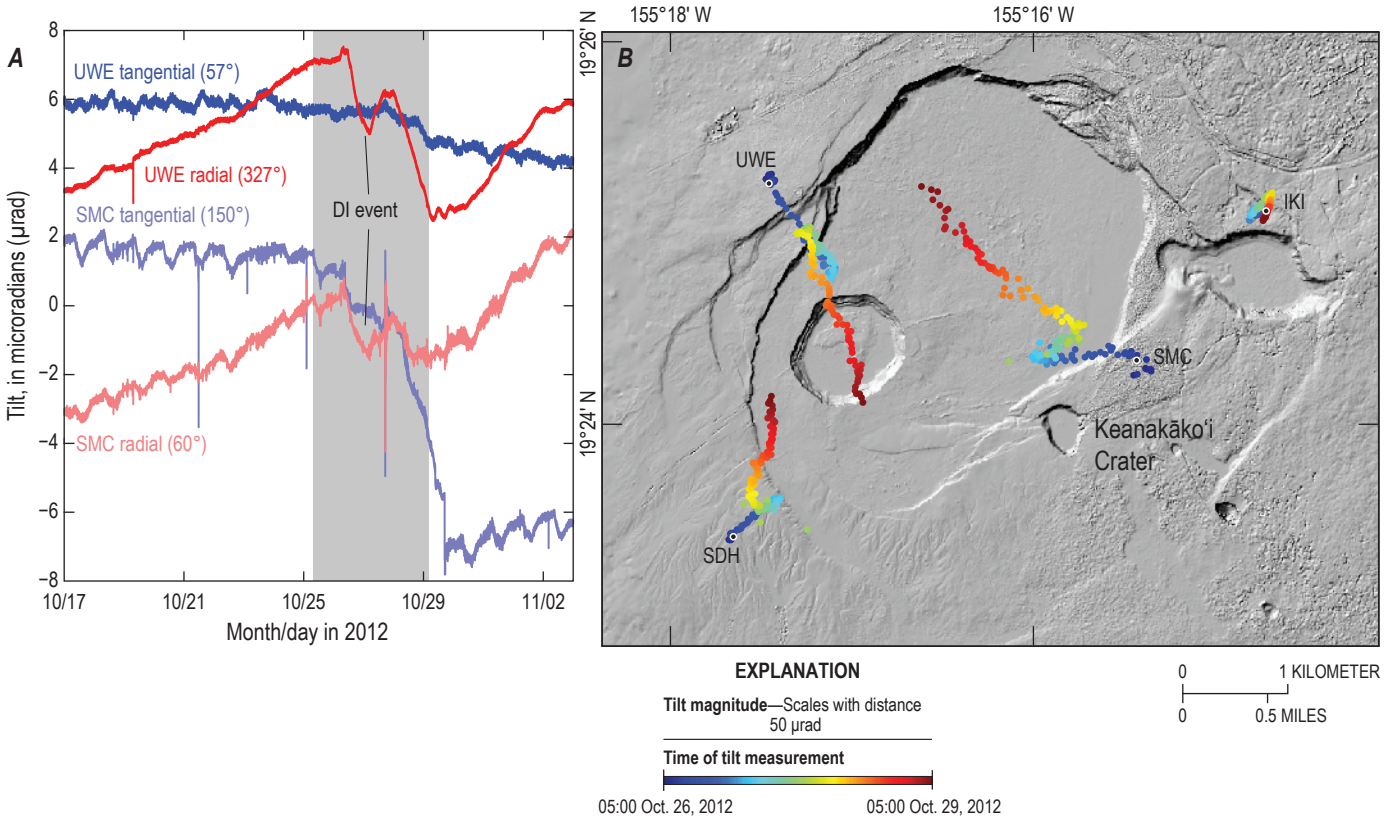


**Figure 14.** Plot and map showing tilt measurements during a possible small intrusion event. *A*, Tilt measured by borehole stations UWE and SMC (locations in fig. 1) in late October and early November 2012. The radial component is oriented toward the main summit deformation source, and the tangential component is orthogonal to that direction. Tilt azimuths are given in degrees. Gray bar indicates time spanned by data in part *B*. After a period of inflation (indicated by positive radial tilt), a deflation-inflation (DI) event occurred on October 26–27, followed by a second event that manifested as deflation at station UWE starting on October 28, but with a strong tangential component at station SMC. This event may have been a small intrusion in the southeast part of the caldera, near Keanakāko‘i Crater. *B*, Map showing the progression of tilt at summit stations between 05:00 a.m. Hawaiian Standard Time (HST) on October 26, 2012, and 05:00 a.m. HST on October 29, 2012. Colors correspond to time, and the length of trails indicates tilt magnitude. Sampling rate (dot spacing) is 30 minutes. Initial tilt directions on October 26–27 (cool colors) reflect a DI event, whereas those on October 28–29 (warm colors), especially at station SMC, may reflect a minor intrusion in the southeast part of the caldera.

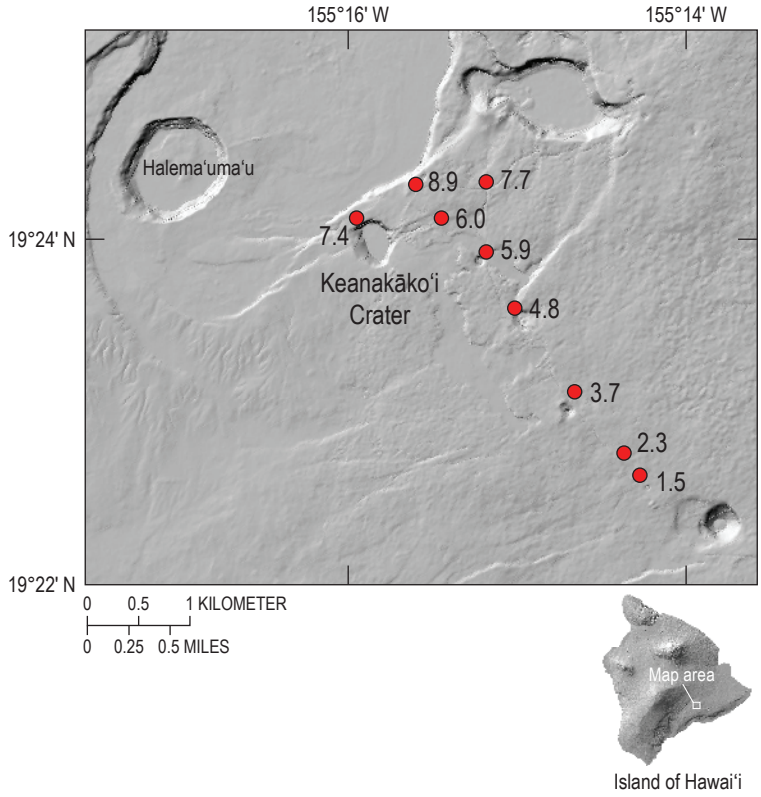


**Figure 15.** Map of vertical changes (in centimeters) from February 2011 to October 31, 2012, based on leveling measurements at benchmarks (red dots) in the upper East Rift Zone. Leveling data are referenced to Global Navigation Satellite System (GNSS) data and have an uncertainty of approximately 1 centimeter (cm). The uplift, which is related to overall inflation of the summit during the nearly 2-year span, decreases with distance from the summit. The area east-northeast of Keanakāko'i Crater, however, shows anomalously high uplift (almost 9 cm) that is not consistent with the expected decrease of uplift magnitude with distance caused by summit inflation, lending circumstantial support to the hypothesis of a sill or plug-like intrusion into this area on October 28–29. White box in location map shows the map area.

Small intrusions at other times are suggested by continuous gravity data. The gravimeter installed at station HOVL-G recorded fluctuations mostly associated with changes in the level of the summit lava lake. During several brief (few days) periods in April 2013, July 2013, and May 2014, observed gravity change far exceeded that which could be caused by lava-level changes in the lake. The May 2014 event was coincident with chaotic tilt signals and a broad increase in shallow seismicity within the summit region, suggesting that the gravity measurement was not a spurious artifact. Given the lack of accompanying coherent deformation, Poland and Carbone (2016) suggested that the May 2014 and similar gravity transient events were related to sudden accumulation of magma in shallow void space near the summit vent and magma conduit, which changed subsurface mass distribution in the vicinity of Halema'uma'u, affecting gravity measurements without causing substantial deformation or lava-level changes. It is difficult to substantiate these conclusions, but the coincidence of multiple geophysical signals is consistent with small, shallow magma accumulation events that might otherwise have gone undetected.

## Summit-Vent Instability

The excellent coverage of Kīlauea's summit region by high-resolution X-band synthetic aperture radar satellites starting in 2008 (fig. 4) made possible the detection and characterization of highly localized deformation associated with instability of the summit eruptive vent during the first years of its existence (Richter and others, 2013). Instability was manifested in X-band interferograms as line-of-sight (LOS) subsidence within about 100 m of the vent rim (fig. 16). Areas closest to the rim subsided fastest, with LOS rates as high as tens of centimeters per year (cm/yr). Higher subsidence rates occurred during periods of rapid vent widening, and little to no subsidence was observed during periods of relative vent stability. Although seemingly inconsequential, the deformation provided an important indicator of heightened potential for rim collapse and associated hazards. Sudden vent rim and wall collapses commonly resulted in explosions when the collapse material impacted the surface of the lava lake (Orr and others, 2013; Patrick and others, 2019b)—events that propelled incandescent material to the rim of Halema'uma'u, presenting a hazard to any nearby people or monitoring infrastructure. Tracking vent instability from InSAR-derived subsidence patterns therefore provided an indication of the potential for rim failure, not unlike the localized deformation seen on unstable lava deltas (Poland and Orr, 2014). During future episodes of lava-lake activity at Kīlauea or elsewhere, high-resolution InSAR may be a valuable tool for monitoring vent-rim stability and evaluating hazard conditions.

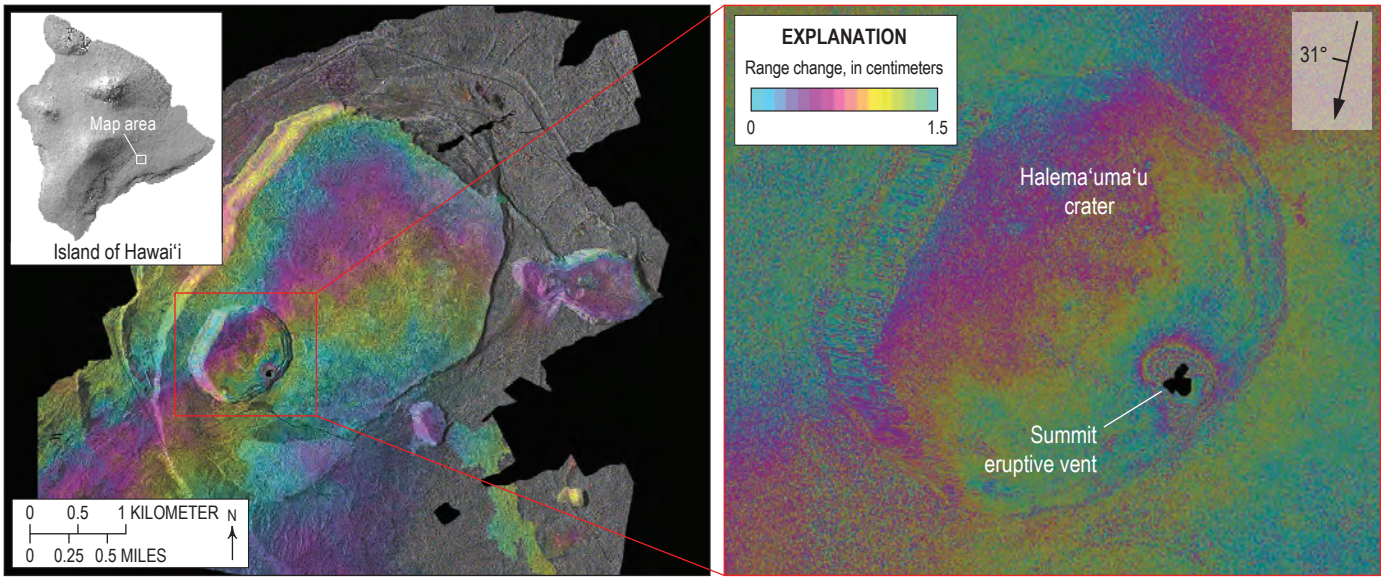


**Figure 16.** TerraSAR-X descending interferogram spanning January 19–April 17, 2009, showing subsidence localized around the summit eruptive vent and indicating vent-rim instability. Modified from Richter and others (2013). White box in location map shows area covered by the interferogram.

# Micro Summit Transient Deformation Events

Another category of smaller transient events exists in addition to the major intrusive/eruptive events, minor intrusions, DI event cycles, and localized vent-rim instability. These “micro” transient events associated with lava lake processes were manifested in tilt and continuous gravity data, and the airborne plume of gas and ash was occasionally detectable in InSAR observations.

## Gas Pistoning

“Gas piston” events are minutes-to-hours-long changes in lava level characterized by a gradual rise and sudden fall in the lava surface. Gas pistoning has been observed both in lava channels and within eruptive vents at Kīlauea and is thought to be driven by shallow gas accumulation in, and sudden release from, the upper part of the lava flow or lava lake (Swanson and others, 1979; Orr and Rea, 2012; Patrick and others, 2016, 2019b).

Gas pistoning during Kīlauea’s 2008–2018 summit eruption was associated with lava-level changes of as much as tens of meters (Patrick and others, 2016, 2019b). The process was cyclic and manifested by a decrease in seismic tremor amplitude, gas flux, spattering, and velocity of lava circulation during lava-level high stands, with a return to normal behavior following rapid lava-level drops. Gas pistoning at Kīlauea appears to be driven by gas accumulation beneath the lava-lake crust, forming a foam layer, as opposed to some deeper process or ascent of gas slugs, as may be the case at other volcanoes (Patrick and others, 2016, 2019b). The formation of a foam is supported by continuous gravity measurements, which indicate only a very slight change in mass despite substantial changes in lava level (fig. 17). Coupling gravity and lava-level data allowed Poland and Carbone (2018) to calculate a density of about 100–200 kg/m$^3$ for the portion of the lava lake involved in gas pistoning (typically the upper 10–30 m).

In general, lava level and deformation at Kīlauea’s summit were directly correlated during the 2008–2018 eruption—lava-level increases were accompanied by summit inflation in response to pressurization, and vice versa (Patrick and others, 2019a,b). Paradoxically, the behavior is anti-correlative during gas pistoning—increases in lava-level height were accompanied by deflation, and vice versa (fig. 17). Relative tilt magnitudes indicate that the deformation source was the shallow Halema‘uma‘u reservoir (Poland and Carbone, 2018). These data indicate that the shallow magma reservoir was reacting passively to pressure changes in the conduit and lava lake, in contrast to periods when deformation and lava-level change were correlative and actively driven by pressure changes in the Halema‘uma‘u magma reservoir.

## Explosions and Very-Long-Period (VLP) Seismicity

Small explosions and very-long-period (VLP) seismic events occurred intermittently throughout the course of the summit eruption (Patrick and others, 2019b; Crozier and Karlstrom, 2021). These events were frequently related, with explosions and VLP seismicity triggered by rim and

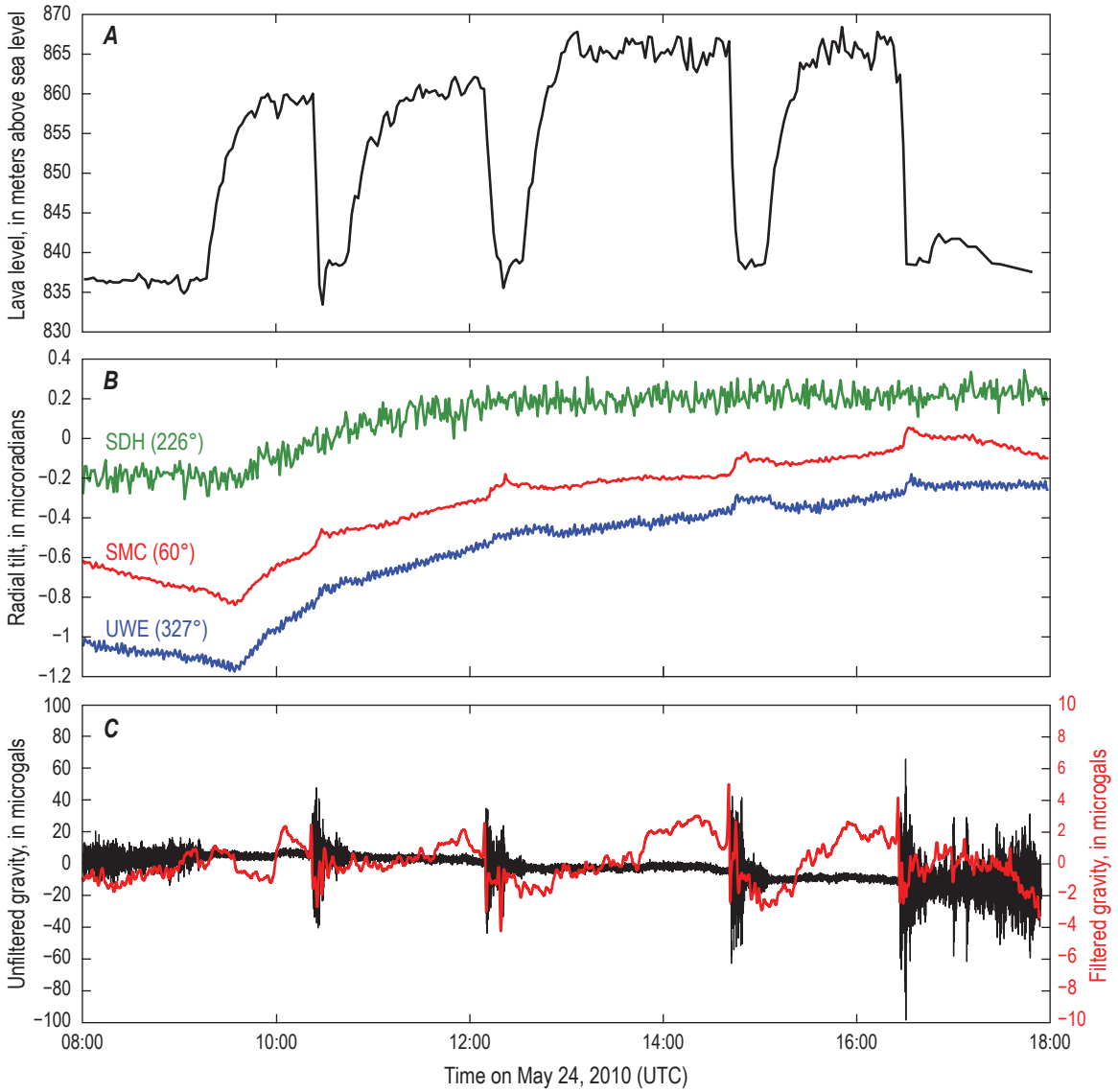


**Figure 17.** Plot of time series variations in (*A*) lava level, (*B*) tilt directed radial to the summit at borehole stations UWE, SMC, and SDH, with tilt azimuth given in degrees, and (*C*) continuous gravity measured at station HOVL-G for a 10-hour period on May 24, 2011 (Coordinated Universal Time [UTC] time). Station locations are shown in figure 1. A band-pass filter with cutoff frequencies of 0.08 and 8 millihertz (mHz; corresponding to periods of 2 to 200 minutes) was applied to the gravity data to isolate the component of the signal related to gas pistoning, creating the filtered time series (red line in part *C*). Gas-piston events are characterized by a rise and plateau in lava level over one to a few hours, then a sudden drop to the original level. Lava-level drops are accompanied by small positive (inflationary) tilts, and lava-level rises by small negative (deflationary) tilts, at stations SMC and UWE, which are closest to the Halema'uma'u magma reservoir. Each lava-level drop is also accompanied by a small decrease in gravity, seen best in the filtered time series. The small gravity change despite the tens of meters of lava-level change implies very small changes in mass, and hence that the portion of the lava lake involved in gas pistoning is very low density—approximately 100–200 kilograms per cubic meter (kg/m$^3$). Modified from Poland and Carbone (2018).

wall collapses impacting the lava-lake surface (Orr and others, 2013). Explosions commonly occurred during the deflation phase of DI events, suggesting that removal of wall support caused by the drop in lava level during deflation led to rim or wall collapses (Patrick and others, 2019b). Explosions and composite seismic events, which included both high-frequency and VLP components, were usually accompanied by sudden vent-radial tilt offsets on summit tiltmeters (fig. 18), with magnitudes usually much less than 1 microradian (although a few events were larger). Why would such processes be accompanied by inflationary tilt jumps? The inflation is consistent with a pressure increase, so one possible explanation is that the explosions and VLP events were associated with rapid vesiculation of the summit lava lake and column. Rapid vesiculation is supported by the agitated, roiling state of the lava lake after such events (Orr and others, 2013). This increase in gas volume would result in a corresponding, but small, increase in pressure

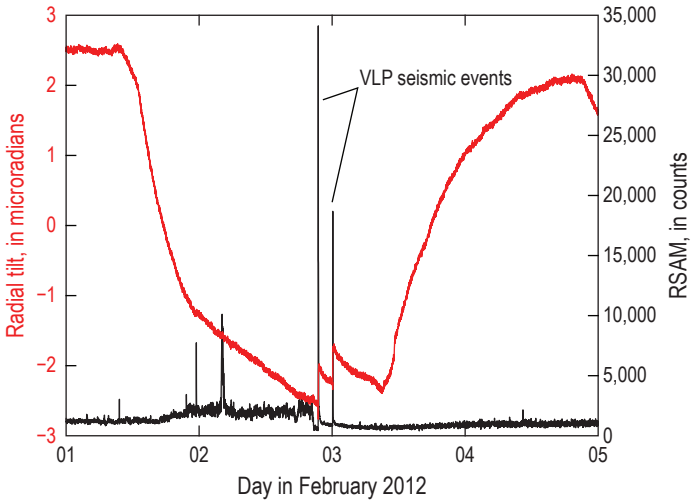


**Figure 18.** Plot of tilt (red line) from the radial (327°) component of borehole instrument UWE, and real-time seismic-amplitude measurement (RSAM; black line) from a collocated broadband seismometer, spanning February 1–4, 2012. During a deflation-inflation (DI) event, a pair of rim collapses late on February 2 and early on February 3 led to rockfalls that impacted the summit lava lake, generating composite seismic events with strong very-long-period (VLP) components and resulting in inflationary tilt offsets. These types of tilt offsets were commonly associated with rim collapses and VLP seismicity, especially in the early years of the summit eruption as the vent expanded, and they commonly occurred during the deflation phases of DI events.

within the magmatic system—VLP source models indicate the Halemaʻumaʻu magma reservoir (for example, Liang and others, 2020)—thereby causing an inflationary jump that subsequently decayed over minutes to hours.

## Eruption-Plume Detection

Although not related to ground deformation or gravity change, InSAR data may have captured signals related to the airborne plume of gas and ash. In some interferograms, a localized phase anomaly is present near the summit eruptive vent (fig. 19). Such anomalies do not resemble deformation patterns associated with any known subsurface source of pressure change, and their spatiotemporal characteristics are never repeated. In this sense they are similar to atmospheric anomalies (for example, Ebmeier and others, 2013), except that in these interferograms there is no correlation between phase change and topography, nor are there similar anomalies in other parts of the interferograms that might indicate a turbulent atmosphere. Given the proximity to the summit vent, we suggest that the anomalous phase change is related to the presence of a gas and ash plume, as has been hypothesized to explain phase changes in interferograms spanning other basaltic eruptions (González and others, 2015). The specific conditions that contributed to the plume being apparent in interferograms are unknown, but they are worthy of further investigation to determine how InSAR may be useful for plume detection and characterization.

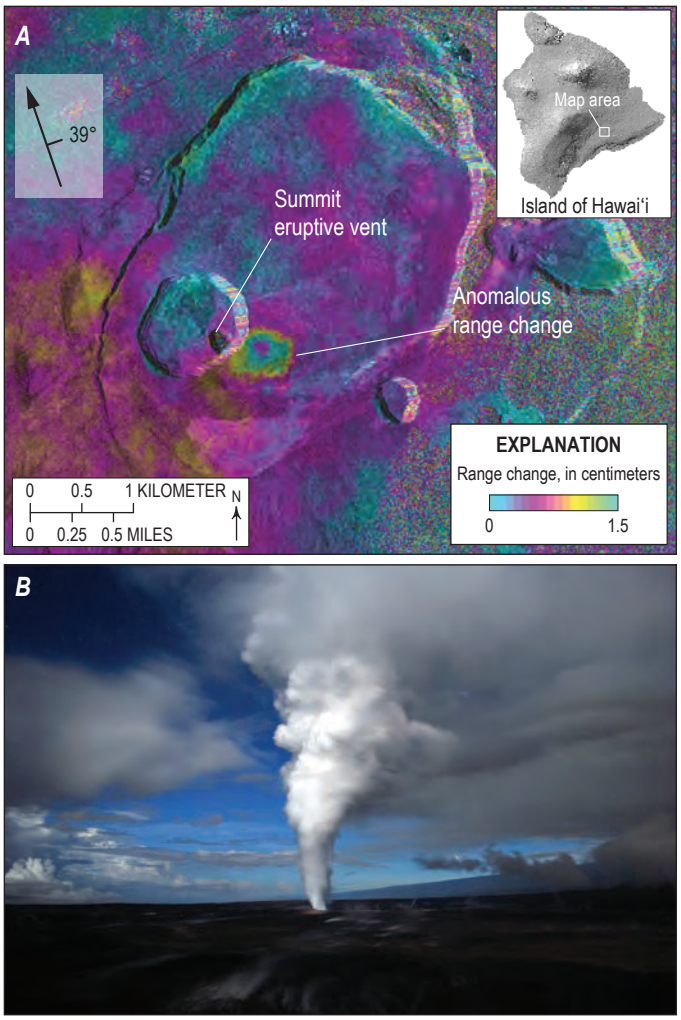


**Figure 19.** Interferogram and photograph showing possible detection of an eruption plume at Kīlauea. *A*, COSMO-SkyMed interferogram spanning February 2–9, 2016, and showing anomalous range change on the east side of Halemaʻumaʻu, adjacent to the summit eruptive vent. The anomaly is not consistent with any other deformation pattern observed at Kīlauea, and its localized character suggests it is not related to weather, but instead may be due to the presence of the summit eruption plume. White box in location map shows the area covered by the interferogram. *B*, Long-exposure nighttime view of the summit eruption plume from the northeast caldera rim looking southwest and showing conditions that might be similar to those that led to the anomalous phase change in the interferogram in part *A*. Photograph taken on November 13, 2008, by Mike Poland.

# Unanswered Questions

Despite all of the data and observations collected over the 10 years of Kīlauea's 2008–2018 summit eruption, a number of fundamental questions remain unanswered. We highlight a few of those questions here, in hopes that future studies might use geodetic and other volcano-monitoring datasets collected during the eruption to help answer some of these known unknowns.

## What Caused the 2008–2018 Summit Eruption?

The immediate mechanism for a volcanic eruption is commonly straightforward—pressure in a magma reservoir eventually overcomes the strength of the host rock, leading to failure of the reservoir roof or wall and magma ascent toward the surface. This pressurization is usually, although not always, accompanied by inflation and increased seismic activity. Recognizing such patterns has long been the primary basis for eruption forecasting (Poland and Anderson, 2020, and references therein). The onset of Kīlauea's 2008–2018 summit eruption, however, occurred during a time of deflation and was characterized by increasing seismic tremor and $SO_2$ emissions (fig. 20) (Wilson and others, 2008). If magma was rising, as suggested by increasing tremor and gas flux, why was Kīlauea not inflating?

One possible explanation is that increased degassing was triggered by Halema'uma'u reservoir depressurization, which led to gases reaming or stoping a pathway to the surface, gas pressure causing the March 19, 2008, explosion, and magma buoyantly rising into the newly created vent. This idea was proposed by Poland and others (2009) based on analogy with the 2007 Father's Day intrusion and eruption on Kīlauea's ERZ (blue line in fig. 20). As magma rapidly drained from beneath the summit to feed the Father's Day dike intrusions and the summit deflated, a paradoxical increase in summit $SO_2$ emissions occurred, with gas flux more than doubling. Poland and others (2009) suggested that rapid depressurization

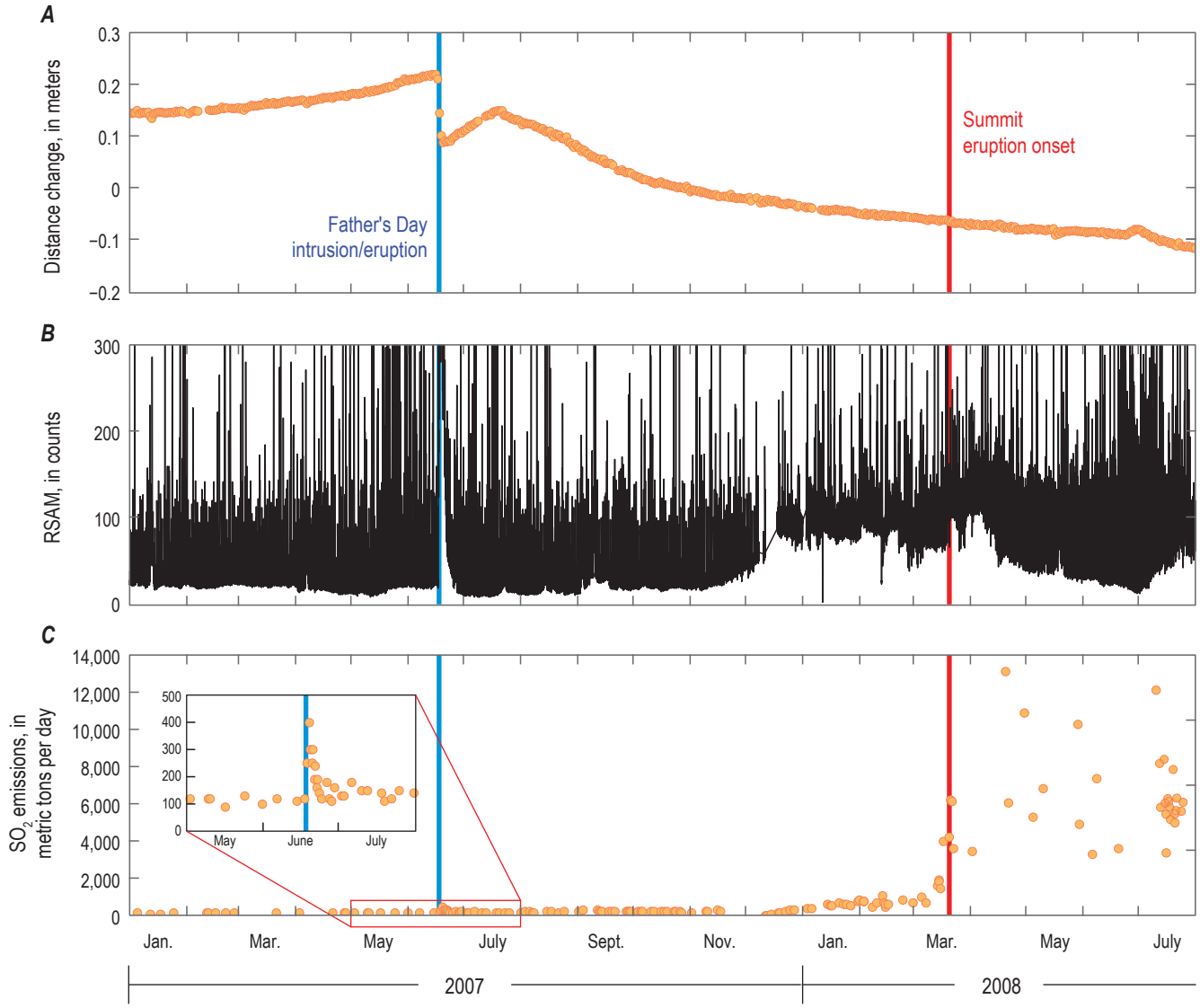


**Figure 20.** Plots of time series variations in summit deformation (*A*), real-time seismic-amplitude measurement (RSAM) (*B*), and $SO_2$ emissions (*C*) spanning January 2007–July 2008. Deformation is represented by the change in distance between Global Navigation Satellite System (GNSS) stations UWEV and AHUP (locations in fig. 1), for which positive change indicates inflation. RSAM is from seismic station RIM, located near GNSS site CRIM (location in fig. 1). Blue line marks the June 17–19 event known as the Father's Day East Rift Zone intrusion and eruption (Poland and others, 2008; Montgomery-Brown and others, 2010). Red line marks the onset of the 2008–2018 summit eruption, defined by the initial explosive opening of the new summit vent within Halema'uma'u.

of the summit magma reservoir caused volatile exsolution. A similar sequence may have played out in the months prior to the summit eruption onset, with persistent deflation indicating depressurization of the summit magma reservoir. The reservoir system had been engorged owing to an increase in magma supply to the volcano during 2003–2007 (Poland and others, 2012); steady pressure loss from this system may have led to the gas release that ultimately resulted in the summit eruption. Although conceivable, such a mechanism is speculative, and the question of the summit eruption initiation mechanism remains worthy of further investigation.

## What Conditions Lead to Summit Intrusions?

Prior to the onset of the Pu‘u‘ō‘ō eruption in 1983, summit intrusions and eruptions were common, especially in the 1960s, 1970s, and early 1980s (for example, Fiske and Kinoshita, 1969; Dvorak and others, 1983; Yang and others, 1992). Once Pu‘u‘ō‘ō formed, however, this decades-long pattern was broken, at least until the onset of the summit eruption in 2008. An intrusion occurred in May 2015, with smaller intrusive events (based on overall deformation) taking place in October 2012, and possibly in April 2013, July 2013, and May 2014. Why did these intrusions occur?

Both the 2012 and 2015 intrusions (discussed above) were preceded by periods of summit inflation, which reflects an imbalance between magma supply and withdrawal. Summit inflation during 2003–2007 was a result of a surge in magma supply to the volcano (Poland and others, 2012; Anderson and Poland, 2016). Other periods of summit inflation have been associated with magma accumulation in the magmatic plumbing system because of decreased lava effusion from ERZ eruptive vents, for example, prior to the 2011 ERZ Kamoamoa fissure eruption and other ERZ eruptive events that year (Orr and others, 2015; Patrick and others, 2019b; fig. 9). The onset of inflation prior to the 2015 intrusion was sudden and not accompanied by a noteworthy change in ERZ eruptive activity, and there was no obvious change in ERZ effusion rate prior to the 2012 intrusion. These observations support the possibility of a short-term increase in magma supply as the mechanism for the summit intrusions—a process also suggested by Patrick and others (2019b) and Bemelmans and others (2021)—although the brief nature of the activity makes it difficult to corroborate that hypothesis.

The 2012 and 2015 intrusions appear to have initiated because of rupture of the south caldera reservoir and were not associated with any changes in ERZ eruptive activity. If there was a temporary increase in magma supply prior to these events, why did that magma not simply enter the ERZ conduit system and feed downrift eruptive vents? In 2015, magma clearly fed the Halema‘uma‘u magma reservoir, where the first inflation was detected (fig. 12*A*), before ultimately causing a rupture from the south caldera reservoir (fig. 12*B*,*C*) (Bemelmans and others, 2021). Perhaps this is a common mode of summit intrusive activity, as might be indicated by deformation patterns associated with past intrusions (for example, Fiske and Kinoshita, 1969; Dvorak and others, 1983). In this sense, further investigation, especially of the well-documented 2015 intrusion (Bemelmans and others, 2021), may shed additional light on the nature of the summit magmatic plumbing system and past intrusions—offering a glimpse into what might occur in the future.

## What Causes Deflation-Inflation Events?

Despite their ubiquitous occurrence, especially during the 2008–2018 summit eruption but also before and after, there remains no consensus on the mechanism for DI events. The increase in the number of DI events with the onset of the summit eruption suggests that they may be related to magma convection and degassing (fig. 13); however, their continued occurrence soon after the 2018 summit collapse, during a period of magma recharge but very low levels of summit degassing, is puzzling (although gas emissions were probably reduced because of scrubbing by the reestablished water table in the summit region). In addition, DI events do not occur regularly in time; there can be weeks-to-months-long periods of no events, and then a series of numerous back-to-back events that do not have an obvious correlation with changes in summit gas emissions. If DI events are instead related to a blockage in the magma system, why is an accumulation of magma behind the blockage, which would cause deep pressurization and broad inflation, not apparent (Anderson and others, 2015; Anderson and others, 2020)? If the blockage was between the two reservoirs, is the south caldera reservoir simply too deep and too large for such changes to be detectable? And why did the nature of DI event manifestation at Pu‘u‘ō‘ō vary so widely, from strongly reflective of summit deformation to completely independent (Anderson and others, 2015)?

Hundreds of DI events of varying size and temporal evolution occurred during the 2008–2018 summit eruption. This incredible record, made possible by comprehensive and long-term geodetic monitoring of the summit region, provides exceptional fodder for fluid mechanical studies that investigate the potential causes of these enigmatic transient events and that use them to better understand the magmatic system. We encourage continued exploration of the nature and driving mechanisms of DI events, which should provide new constraints on magma plumbing and transport beneath Kīlauea’s summit region.

## What is the Geometry of Summit Magma Storage?

The current conceptual model of the summit magma system involves at least two major magma storage areas, the Halema‘uma‘u and south caldera reservoirs, which provide magma to the volcano’s two rift systems and, during 2008–2018, to the summit vent. The Halema‘uma‘u magma reservoir, which fed the summit vent and lava lake, is the more dynamic of the two, responding on time scales of hours to days to transient events like ERZ eruptive activity and DI events, whereas the south caldera reservoir experiences more gradual changes in pressure over weeks to years (although we recognize bias in this observation, given the greater depth of

the south caldera reservoir and consequent challenge of detecting small changes). The best-constrained volume estimate of the Halemaʻumaʻu magma reservoir is 2.5 to 7.2 $km^3$ (68 percent confidence level) based on modeling of geodetic and lava-lake observations acquired during the opening phases of the 2018 summit collapse (Anderson and others, 2019). The south caldera reservoir is probably larger—at least 10 $km^3$ (for example, Poland and others, 2014)—but the volume is poorly constrained.

One model for the Halemaʻumaʻu reservoir depicts it as an offshoot of the south caldera reservoir (Poland and others, 2014; fig. 3). But are these reservoirs really connected in this way? Evidence is contradictory.

Over much of the decade-long summit eruption, the Halemaʻumaʻu and south caldera magma reservoirs acted in concert, pressurizing and depressurizing together and therefore suggesting some level of connectivity. Deformation during the 2015 summit intrusion (fig. 12) would also seem to indicate that the reservoirs are connected, since magma drained from the Halemaʻumaʻu source to feed the intrusion emanating from the south caldera reservoir (Bemelmans and others, 2021). A strong connection is favored by petrologic evidence as well, given that lava flows erupted in the lower ERZ in 2018 included crystals that formed in both the Halemaʻumaʻu and south caldera reservoirs (Wieser and others, 2021).

Other time periods suggest that the connection between the two storage areas is not always robust. During late 2011 through 2012, the Halemaʻumaʻu and south caldera reservoirs acted independently, with one inflating while the other deflated (figs. 5, 7). And even during the 2015 intrusion, magma drained from the Halemaʻumaʻu reservoir for about a day before the intrusion was strongly manifested (Bemelmans and others, 2021). Anderson and others (2020) examined DI events and pointed out that south caldera inflation does not accompany Halemaʻumaʻu deflation, which might be expected if magma were backing up behind some blockage, or if magma was flushing from shallow to deeper levels (fig. 13), although this assumes a mechanism for DI events that is unsubstantiated. Observations during the 2018 lower ERZ eruption and summit collapse also call into question a direct connection. Pressure changes due to summit-collapse events propagated rapidly from the summit to the lower ERZ, resulting in the onset of effusive surges within minutes, and peaking after hours (Patrick and others, 2019c). Such a strong connection between the summit source and the lower ERZ, 40 km away, seems improbable if those pressure changes were buffered by the south caldera reservoir, and physics-based models indicate that a shallow ERZ conduit connected to the Halemaʻumaʻu source is far more conductive hydraulicly (Wang and others, 2021). The surges, along with models of magma flux and summit deformation, suggest the possibility of a direct ERZ connection from the Halemaʻumaʻu reservoir, instead of the south caldera reservoir as envisioned by Poland and others (2014). Some evidence thus supports the pioneering study of DI events by Cervelli and Miklius (2003), who suggested that the ERZ and Halemaʻumaʻu magma reservoir were directly linked.

Geodetic data collected before, during, and after Kīlauea's 2008–2018 summit eruption certainly highlight the complexity of the summit magmatic plumbing system. The existence of at least two storage areas beneath Kīlauea's summit is unequivocal. Details of their location, character, and relation to one another, and even to the rift zones and other magmatic pathways in the summit region, however, remain unclear and are worthy of continuing scrutiny. Ultimately, understanding these storage systems is critical for improving forecasts of eruptive activity.

## What is the Nature of Void Space—If it Exists—Beneath the Summit?

A consistent theme in microgravity studies of Kīlauea is the existence of void space in the upper few kilometers beneath the summit. Dzurisin and others (1980) were the first to suggest this, arguing that void space was created during magma drainage from the summit associated with the 1975 Kalapana earthquake because the mass loss from beneath the caldera was greater than that which could be explained by the surface deformation. Gravity surveys through early 2008 returned to this mechanism, arguing that mass increases in the absence of surface uplift were best explained by magma accumulation in void space—perhaps the very void space that had been created in 1975. The filling of this space, albeit uncertain given summit eruptions in 1982, may have ultimately culminated in the 2008–2018 summit eruption (Johnson and others, 2010). Filling of void space has also been invoked to explain short-term gravity changes recorded by the continuous gravimeter at station HOVL-G (fig. 1) that may indicate small intrusions near the 2008–2018 summit eruptive vent (Poland and Carbone, 2016). Finally, filling of void space by magma is invoked as the mechanism for the gravity increase observed in the months after the 2018 summit collapse—a gravity increase that was followed within months by surface uplift, suggesting the accessible void space had been filled to the point that pressurization could be sustained (Poland and others, 2019).

It is reasonable to question the existence of void space beneath Kīlauea's summit were the hypothesis based on gravity data alone. Geologic evidence, however, also indicates that void space is present. For example, Houghton and others (2011) noted that the volume of the ejecta from the March 19, 2008, explosion at the onset of the summit eruption was less than 1 percent of the volume of the source pit crater. This observation implies that a cavity of some kind was already present beneath the ground prior to the eruption, and that the March 19 explosion merely exposed this void space to the surface. Given the heavily fractured nature of the caldera floor and its numerous collapses of varying sizes over the past 200 years (Wright and Klein, 2014), the interlayering of ash and lava flows of varying textures at depth, the interconnectivity of the groundwater system (for example, Keller and others, 1979), and the degree of subsurface hydrothermal alteration (Gailler and others, 2019), there can be little doubt that open fractures and voids exist beneath the surface.

Collectively, void space beneath Kīlauea's summit probably exists as a network of interconnected cracks and interstitial spaces, rather than a single or a few cavernous volumes. Dzurisin and others (1980) modeled void creation of 40–90 $\times 10^6$ $m^3$ as a result of the 1975 coseismic magma drainage, whereas Johnson and others (2010) suggested filling of 21–120 $\times 10^6$ $m^3$ of void space during 1975–2008. Models of gravity data indicate that the voids are in close proximity to the Halema'uma'u magma reservoir, which is unsurprising given the dynamic nature of magma storage in that region, the hydrothermal alteration zones nearby, and changing groundwater conditions. It is likely that the creation and filling of void space within the upper 1–2 km beneath Kīlauea's summit is a persistent process, given the frequent cycles of magmatic resurgence and collapse. This being the case, gravity measurements are an especially important means of assessing the state of magmatic activity, as pointed out by Poland and others (2019).

## Summary and Conclusions

The onset of Kīlauea's summit eruption in 2008 motivated a rapid increase in the number and type of geodetic monitoring instruments, especially GNSS, to capture processes and changes associated with the first prolonged summit lava lake at the volcano since 1968. It also occurred during a period of rapid technological innovation, enabling the application of emerging geodetic monitoring techniques, like continuous gravity. Furthermore, it occurred when an impressive number of InSAR-capable satellites were orbiting Earth. The resulting data from this surge of geodetic monitoring have provided insights into a range of geophysical processes, spanning timescales from seconds to years and magnitudes from micrometers to meters.

During the decade of eruptive activity, long-term deformation at Kīlauea's summit evolved gradually from deflation before 2010 to inflation after 2013. This broad change appears to have been associated with variable rates of magma supply from the mantle source area to the volcano's summit magma reservoirs, as well as changes in the efficiency of magma flow to the volcano's ERZ eruptive vent. Superimposed on these long-term changes were transients of various spatiotemporal scales. The most significant events included intrusions beneath the summit and new eruptive outbreaks along the ERZ that affected summit deformation, with precursory inflation, accompanying deflation, and subsequent reinflation. Geodetic data also imaged small-scale processes, like days-long episodic deflation-inflation events, gas-piston cycles, small explosions from the lava lake, and instability of the summit vent rim. InSAR data also recorded signals possibly reflecting the summit's plume of gas and ash. Many of these phenomena would not have been detectable without the dense array of sensitive geodetic instrumentation in Kīlauea's summit region and the imagery provided by an extensive constellation of synthetic aperture radar satellites. This incredible record of geodetic change can continue to shed light on numerous remaining questions about Kīlauea's 2008–2018 summit eruption, such as its original triggering mechanism, the causes and manifestations of intrusions of varying sizes, the driving forces behind deflation-inflation events, the geometry of magma storage, and the existence of void space at depth. We are hopeful that these and other questions will be addressed by future research that exploits, and builds on, the vast archive of geodetic and other observations from Kīlauea's summit during this important period of the volcano's history.

## References Cited

Anderson, A.N., Foster, J.H., and Frazer, N., 2020, Implications of deflation-inflation event models on Kīlauea Volcano, Hawai'i: Journal of Volcanology and Geothermal Research, v. 397, article no. 106832, https://doi.org/10.1016/j.jvolgeores.2020.106832.

Anderson, K.R., Johanson, I.A., Patrick, M.R., Mengyang, G., Segall, P., Poland, M.P., Montgomery-Brown, E.K., and Miklius, A., 2019, Magma reservoir failure and the onset of caldera collapse at Kīlauea Volcano in 2018: Science, v. 366, no. 6470, article no. eaaz1822, https://doi.org/10.1126/science.aaz1822.

Anderson, K.R., and Poland, M.P., 2016, Bayesian estimation of magma supply, storage, and eruption rates using a multiphysical volcano model—Kīlauea Volcano, 2000–2012: Earth and Planetary Science Letters, v. 447, p. 161–171, https://doi.org/10.1016/j.epsl.2016.04.029.

Anderson, K.R., Poland, M.P., Miklius, A., and Johnson, J.H., 2015, Episodic deflation–inflation events at Kīlauea Volcano and implications for the shallow magma system, *in* Carey, R.J., Cayol, V., Poland, M.P., and Weis, D., eds., Hawaiian Volcanoes from Source to Surface: American Geophysical Union Monograph 208, p. 229–250, https://doi.org/10.1002/9781118872079.ch11.

Bagnardi, M., Poland, M.P., Carbone, D., Baker, S., Battaglia, M., and Amelung, F., 2014, Gravity changes and deformation at Kīlauea Volcano, Hawaii, associated with summit eruptive activity, 2009–2012: Journal of Geophysical Research, v. 119, no. 9, p. 7288–7305, https://doi.org/10.1002/2014JB011506.

Baker, S., and Amelung, F., 2012, Top-down inflation and deflation at the summit of Kīlauea Volcano, Hawai'i observed with InSAR: Journal of Geophysical Research, v. 117, article no. B12406, https://doi.org/10.1029/2011JB009123.

Bemelmans, M.J.W., de Zeeuw-van Dalfsen, E., Poland, M.P., and Johanson, I.A., 2021, Insight into the May 2015 summit inflation event at Kīlauea Volcano, Hawai'i: Journal of Volcanology and Geothermal Research, v. 415, article no. 107250, https://doi.org/10.1016/j.jvolgeores.2021.107250.

Carbone, D., and Poland, M.P., 2012, Gravity fluctuations induced by magma convection at Kīlauea Volcano, Hawai'i: Geology, v. 40, no. 9, p. 803–806, https://doi.org/10.1130/G33060.1.

Carbone, D., Poland, M.P., Patrick, M.R., and Orr, T.R., 2013, Continuous gravity measurements reveal a low-density lava lake at Kīlauea Volcano, Hawai'i: Earth and Planetary Science Letters, v. 376, p. 178–185, https://doi.org/10.1016/j.epsl.2013.06.024.

Carey, R.J., Manga, M., Degruyter, W., Gonnermann, H., Swanson, D., Houghton, B., Orr, T., and Patrick, M., 2013, Convection in a volcanic conduit recorded by bubbles: Geology, v. 41, no. 4, p. 395–398, https://doi.org/10.1130/G33685.1.

Carey, R.J., Manga, M., Degruyter, W., Swanson, D., Houghton, B., Orr, T., and Patrick, M., 2012, Externally triggered renewed bubble nucleation in basaltic magma—The 12 October 2008 eruption at Halema'uma'u Overlook vent, Kīlauea, Hawai'i, USA: Journal of Geophysical Research, v. 117, article no. B11202, https://doi.org/10.1029/2012JB009496.

Cervelli, P.F., and Miklius, A., 2003, The shallow magmatic system of Kīlauea volcano, *in* Heliker, C., Swanson, D.A., and Takahashi, T.J., eds., The Pu'u 'Ō'ō-Kūpaianaha eruption of Kīlauea Volcano, Hawai'i; the first 20 years: U.S. Geological Survey Professional Paper 1676, p. 149–163, https://doi.org/10.3133/pp1676.

Cervelli, P., Segall, P., Amelung, F., Garbeil, H., Meertens, C., Owen, S., Miklius, A., and Lisowski, M., 2002, The 12 September 1999 upper East Rift Zone dike intrusion at Kilauea Volcano, Hawaii: Journal of Geophysical Research, v. 107, article no. B7, 13 p., https://doi.org/10.1029/2001JB000602.

Conway, S., Wauthier, C., Fukushima, Y., and Poland, M., 2018, A retrospective look at the February 1993 east rift zone intrusion at Kīlauea volcano, Hawaii: Journal of Volcanology and Geothermal Research, v. 358, p. 241–251, https://doi.org/10.1016/j.jvolgeores.2018.05.017.

Crozier, J., and Karlstrom, L., 2021, Wavelet-based characterization of very-long-period seismicity reveals temporal evolution of shallow magma system over the 2008–2018 eruption of Kīlauea Volcano: Journal of Geophysical Research, v. 126, no. 6, https://doi.org/10.1029/2020JB020837.

Davis, P.M., 1986, Surface deformation due to inflation of an arbitrarily oriented triaxial ellipsoidal cavity in an elastic half-space, with reference to Kilauea Volcano, Hawaii: Journal of Geophysical Research, v. 91, article no. B7, p. 7429–7438, https://doi.org/10.1029/JB091iB07p07429.

Decker, R.W., Hill, D.P., and Wright, T.L., 1966, Deformation measurements on Kilauea Volcano, Hawai'i: Bulletin Volcanologique, v. 29, p. 721–731, https://doi.org/10.1007/BF02597190.

Decker, R.W., Okamura, A., Miklius, A., and Poland, M., 2008, Evolution of deformation studies on active Hawaiian volcanoes: U.S. Geological Survey Scientific Investigations Report 2008–5090, 23 p., https://doi.org/10.3133/sir20085090.

Dvorak, J., Okamura, A., and Dieterich, J.H., 1983, Analysis of surface deformation data, Kilauea Volcano, Hawaii, October 1966 to September 1970: Journal of Geophysical Research, v. 88, article no. B11, p. 9295–9304, https://doi.org/10.1029/JB088iB11p09295.

Dzurisin, D., Anderson, L.A., Eaton, G.P., Koyanagi, R.Y., Lipman, P.W., Lockwood, J.P., Okamura, R.T., Puniwai, G.S., Sako, M.K., and Yamashita, K.M., 1980, Geophysical observations of Kilauea Volcano, Hawaii; 2. Constraints on the magma supply during November 1975–September 1977, *in* McBirney, A.R. ed., Gordon A. Macdonald memorial volume: Journal of Volcanology and Geothermal Research, v. 7, nos. 3–4, p. 241–269, https://doi.org/10.1016/0377-0273(80)90032-3.

Dzurisin, D., and Poland, M.P., 2018, Magma supply to Kīlauea Volcano, Hawai'i, from inception to now—Historical perspective, current state of knowledge, and future challenges, *in* Poland, M.P., Garcia, M.O., Camp, V.E., and Grunder, A., eds., Field volcanology—A tribute to the distinguished career of Don Swanson: Geological Society of America Special Paper 538, p. 275–295, https://doi.org/10.1130/2018.2538(12).

Eaton, J.P., 1959, A portable water-tube tiltmeter: Bulletin of the Seismological Society of America, v. 49, no. 4, p. 301–316.

Eaton, J.P., and Murata, K.J., 1960, How volcanoes grow: Science, v. 132, article no. 3432, p. 925–938, https://doi.org/10.1126/science.132.3432.925.

Ebmeier, S.K., Biggs, J., Mather, T.A., and Amelung, F., 2013, On the lack of InSAR observations of magmatic deformation at Central American volcanoes: Journal of Geophysical Research, v. 118, no. 5, p. 2571–2585, https://doi.org/10.1002/jgrb.50195.

Fiske, R.S., and Kinoshita, W.T., 1969, Inflation of Kilauea Volcano prior to its 1967–1968 eruption: Science, v. 165, article no. 3891, p. 341–349, https://doi.org/10.1126/science.165.3891.341.

Gailler, L., Kauahikaua, J., Lénat, J.-F., Revil, A., Gresse, M., Ahmed, A.S., Cluzel, N., Manthilake, G., Gurioli, L., Johnson, T., Finizola, A., and Delcher, E., 2019, 3D electrical conductivity imaging of Halema'uma'u lava lake (Kīlauea volcano): Journal of Volcanology and Geothermal Research, v. 381, p. 185–192, https://doi.org/10.1016/j.jvolgeores.2019.06.001.

González, P.J., Bagnardi, M., Hooper, A.J., Larsen, Y., Marinkovic, P., Samsonov, S.V., and Wright, T.J., 2015, The 2014–2015 eruption of Fogo volcano—Geodetic modelling of Sentinel-1 TOPS interferometry: Geophysical Research Letters, v. 42, no. 21, p. 9239–9246, https://doi.org/10.1002/2015GL066003.

Heliker, C., and Mattox, T.N., 2003, The first two decades of the Pu‘u ‘Ō‘ō-Kūpaianaha eruption; chronology and selected bibliography, in Heliker, C., Swanson, D.A., and Takahashi, T.J., eds., The Pu‘u ‘Ō‘ō-Kūpaianaha eruption of Kīlauea Volcano, Hawai‘i; the first 20 years: U.S. Geological Survey Professional Paper 1676, p. 1–27, https://doi.org/10.3133/pp1676.

Helz, R.T., Clague, D.A., Sisson, T.W., and Thornber, C.R., 2014, Petrologic insights into basaltic volcanism at historically active Hawaiian volcanoes, *in* Poland, M.P., Landowski, C.M., and Takahashi, T.J., eds., Characteristics of Hawaiian Volcanoes: U.S. Geological Survey Professional Paper 1801, p. 237–292, https://doi.org/10.3133/pp1801.

Houghton, B.F., Swanson, D.A., Carey, R.J., Rausch, J., and Sutton, A.J., 2011, Pigeonholing pyroclasts—Insights from the 19 March 2008 explosive eruption of Kilauea volcano: Geology, v. 39, no. 3, p. 263–266, https://doi.org/10.1130/G31509.1.

Jachens, R.C. and Eaton, G.P., 1980, Geophysical observations of Kilauea volcano, Hawaii, 1. Temporal gravity variations related to the 29 November, 1975, M = 7.2 earthquake and associated summit collapse: Journal of Volcanology and Geothermal Research, v. 7, no. 3–4, p. 225–240, https://doi.org/10.1016/0377-0273(80)90031-1.

Jaggar, T.A., Jr., and Finch, R.H., 1929, Tilt records for thirteen years at the Hawaiian Volcano Observatory: Bulletin of the Seismological Society of America, v. 19, no. 1, p. 38–51.

Jo, M-J., Jung, H-S., and Won, J-S., 2015, Detecting the source location of recent summit inflation via three-dimensional InSAR observation of Kīlauea Volcano: Remote Sensing, v. 7, no. 11, p. 14386–14402, https://doi.org/10.3390/rs71114386.

Johnson, D.J., Eggers, A.A., Bagnardi, M., Battaglia, M., Poland, M.P., and Miklius, A., 2010, Shallow magma accumulation at Kīlauea Volcano, Hawai‘i, revealed by microgravity surveys: Geology, v. 38, no. 12, p. 1139–1142, https://doi.org/10.1130/G31323.1.

Johnson, J.H., Poland, M.P., Anderson, K.R., and Biggs, J., 2019, A cautionary tale of topography and tilt from Kīlauea Caldera: Geophysical Research Letters, v. 46, no. 8, p. 4221–4229, https://doi.org/10.1029/2018GL081757.

Keller, G.V., Grose, L.T., Murray, J.C., and Skokan, C.K., 1979, Results of an experimental drill hole at the summit of kilauea volcano, Hawaii: Journal of Volcanology and Geothermal Research, v. 5, no. 3–4, p. 345–385, https://doi.org/10.1016/0377-0273(79)90024-6.

Liang, C., Crozer, J, Karlstrom, L., and Dunham, E M., 2020, Magma oscillations in a conduit-reservoir system, application to very long period (VLP) seismicity at basaltic volcanoes; 2. Data inversion and interpretation at Kīlauea Volcano: Journal of Geophysical Research, v. 125, no. 1, article no. e2019JB017456, https://doi.org/10.1029/2019JB017456.

Lundgren, P., Poland, M., Miklius, A., Orr, T., Yun, S.-H., Fielding, E., Liu, Z., Tanaka, A., Szeliga, W., Hensley, S., and Owen, S., 2013, Evolution of dike opening during the March 2011 Kamoamoa fissure eruption, Kīlauea Volcano, Hawai‘i: Journal of Geophysical Research, v. 118, no. 3, p. 897–914, https://doi.org/10.1002/jgrb.50108.

Montgomery-Brown, E.K., and Miklius, A., 2021, Periodic dike intrusions at Kīlauea volcano, Hawai’i: Geology, v. 49, no. 4, p. 397–401, https://doi.org/10.1130/G47970.1.

Montgomery-Brown, E.K., Sinnett, D.K., Poland, M., Segall, P., Orr, T., Zebker, H., and Miklius, A., 2010, Geodetic evidence for en echelon dike emplacement and concurrent slow-slip during the June 2007 intrusion and eruption at Kīlauea volcano, Hawaii: Journal of Geophysical Research, v. 115, article no. B07405, 15 p., https://doi.org/10.1029/2009JB006658.

Neal, C.A., Brantley, S.R., Antolik, L., Babb, J., Burgess, M., Calles, K., Cappos, M., Chang, J.C., Conway, S., Desmither, L., Dotray, P., Elias, T., Fukunaga, P., Fuke, S., Johanson, I.A., Kamibayashi, K., Kauahikaua, J., Lee, R.L., Pekalib, S., Miklius, A., Million, W., Moniz, C.J., Nadeau, P.A., Okubo, P., Parcheta, C., Patrick, M.R., Shiro, B., Swanson, D.A., Tollett, W., Trusdell, F., Younger, E.F., Zoeller, M.H., Montgomery-Brown, E.K., Anderson, K.R., Poland, M.P., Ball, J., Bard, J., Coombs, M., Dietterich, H.R., Kern, C., Thelen, W.A., Cervelli, P.F., Orr, T., Houghton, B.F., Gansecki, C., Hazlett, R., Lundgren, P., Diefenbach, A.K., Lerner, A.H., Waite, G., Kelly, P., Clor, L., Werner, C., Mulliken, K., and Fisher, G., 2019, The 2018 rift eruption and summit collapse of Kīlauea Volcano: Science, v. 363, no. 6425, p. 367–374, https://doi.org/10.1126/science.aav7046.

Orr, T.R., Poland, M.P., Patrick, M.R., Thelen, W.A., Sutton, A.J., Elias, T., Thornber, C.R., Parcheta, C., and Wooten, K.M., 2015, Kīlauea’s 5–9 March 2011 Kamoamoa fissure eruption and its relation to 30+ years of activity from Pu‘u ‘O‘o, *in* Carey, R.J., Cayol, V., Poland, M.P., and Weis, D., eds., Hawaiian volcanoes from source to surface: American Geophysical Union Monograph 208, p. 393–420, https://doi.org/10.1002/9781118872079.ch18.

Orr, T.R., and Rea, J.C., 2012, Time-lapse camera observations of gas piston activity at Pu‘u ‘Ō‘ō, Kīlauea volcano, Hawai‘i: Bulletin of Volcanology, v. 74, no. 10, p. 2353–2362, https://doi.org/10.1007/s00445-012-0667-0.

Orr, T.R., Thelen, W.A., Patrick, M.R., Swanson, D.A., and Wilson, D.C., 2013, Explosive eruptions triggered by rockfalls at Kīlauea volcano, Hawai‘i: Geology, v. 41, no. 2, p. 207–210, https://doi.org/10.1130/G33564.1.

Owen, S., Segall, P., Lisowski, M., Miklius, A., Murray, M., Bevis, M., and Foster, J., 2000, January 30, 1997 eruptive event on Kilauea Volcano, Hawaii, as monitored by continuous GPS: Geophysical Research Letters, v. 27, no. 17, p. 2757–2760, https://doi.org/10.1029/1999GL008454.

Patrick, M.R., Anderson, K.R., Poland, M.P., Orr, T.R., and Swanson, D.A., 2015, Lava lake level as a gauge of magma reservoir pressure and eruptive hazard: Geology, v. 43, no. 9, p. 831–834, https://doi.org/10.1130/G36896.1.

Patrick, M.R., Dietterich, H.R., Lyons, J.J., Diefenbach, A.K., Parcheta, C., Anderson, K.R., Namiki, A., Sumita, I., Shiro, B., and Kauahikaua, J.P., 2019c, Cyclic lava effusion during the 2018 eruption of Kīlauea Volcano: Science, v. 366, no. 6470, article no. eaay9070, https://doi.org/10.1126/science.aay9070.

Patrick, M., Orr, T., Anderson, K., and Swanson, D., 2019a, Eruptions in sync—Improved constraints on Kilauea Volcano's hydraulic connection: Earth and Planetary Science Letters, v. 506, p. 50–61, https://doi.org/10.1016/j.epsl.2018.11.030.

Patrick, M.R., Orr, T., Sutton, A.J., Lev, E., Thelen, W., and Fee, D., 2016, Shallowly driven fluctuations in lava lake outgassing (gas pistoning), Kīlauea Volcano: Earth and Planetary Science Letters, v. 433, no. 1, p. 326–338, https://doi.org/10.1016/j.epsl.2015.10.052.

Patrick, M.R., Orr, T., Swanson, D.A., Houghton, B., Wooten, K., Desmither, L., Parcheta, C., and Fee, D., 2021, Kīlauea's 2008–2018 summit lava lake—Chronology and eruption insights, chap. A *of* Patrick, M., Orr, T., Swanson, D., and Houghton, B., eds., The 2008–2018 summit lava lake at Kīlauea Volcano, Hawai'i: U.S. Geological Survey Professional Pater 1867, 50 p., https://doi.org/10.3133/pp1867A.

Patrick, M., Swanson, D., and Orr, T., 2019b, A review of controls on lava lake level—Insights from Halema'uma'u Crater, Kīlauea Volcano: Bulletin of Volcanology, v. 81, no. 3, article no. 13, https://doi.org/10.1007/s00445-019-1268-y.

Poland, M.P., 2014, Time-averaged discharge rate of subaerial lava at Kīlauea Volcano, Hawai'i, measured from TanDEM-X interferometry—Implications for magma supply and storage during 2011–2013: Journal of Geophysical Research, v. 119, no. 7, p. 5464–5481, https://doi.org/10.1002/2014JB011132.

Poland, M., and Anderson, K.R., 2020, Partly cloudy with a chance of lava flows—Forecasting volcanic eruptions in the 21st century: Journal of Geophysical Research Solid Earth, v. 125, no. 1, article no. e2018JB016974, https://doi.org/10.1029/2018JB016974.

Poland, M.P., and Carbone, D., 2016, Insights into shallow magmatic processes at Kīlauea Volcano, Hawai'i, from a multi-year continuous gravity time series: Journal of Geophysical Research Solid Earth, v. 121, no. 7, p. 5477–5492, https://doi.org/10.1002/2016JB013057.

Poland, M.P., and Carbone, D., 2018, Continuous gravity and tilt reveal anomalous pressure and density changes associated with gas pistoning within the summit lava lake of Kīlauea Volcano, Hawai'i: Geophysical Research Letters, v. 45, no. 5, p. 2319–2327, https://doi.org/10.1002/2017GL076936.

Poland, M.P., Carbone, D., and Patrick, M.R., 2021, Onset and evolution of Kīlauea's 2018 flank eruption and summit collapse from continuous gravity: Earth and Planetary Science Letters, v. 567, no. 117003, https://doi.org/10.1016/j.epsl.2021.117003.

Poland, M.P., Miklius, A., and Montgomery-Brown, E.K., 2014, Magma supply, storage, and transport at shield-stage Hawaiian volcanoes, *in* Poland, M.P., Landowski, C.M., and Takahashi, T.J., eds., Characteristics of Hawaiian volcanoes: U.S. Geological Survey Professional Paper 1801, p. 179–234, https://doi.org/10.3133/pp1801.

Poland, M.P., Miklius, A., Orr, T., Sutton, A.J., Thornber, C.R., and Wilson, D., 2008, New episodes of volcanism at Kilauea Volcano, Hawaii: Eos, American Geophysical Union Transactions, v. 89, no. 5, p. 37–38, https://doi.org/10.1029/2008EO050001.

Poland, M.P., Miklius, A., Sutton, A.J., and Thornber, C.R., 2012, A mantle-driven surge in magma supply to Kīlauea Volcano during 2003–2007: Nature Geoscience, v. 5, no. 4, p. 295–300, supplementary material 16 p., https://doi.org/10.1038/ngeo1426.

Poland, M.P., and Orr, T.R., 2014, Identifying hazards associated with lava deltas: Bulletin of Volcanology, v. 76, no. 12, article no. 880, https://doi.org/10.1007/s00445-014-0880-0.

Poland, M.P., Sutton, A.J., and Gerlach, T.M., 2009, Magma degassing triggered by static decompression at Kīlauea Volcano, Hawai'i: Geophysical Research Letters, v. 36, no. L16306, 5 p., https://doi.org/10.1029/2009GL039214.

Poland, M.P., Zeeuw-van Dalfsen, E., Bagnardi, M., and Johanson, I.A., 2019, Post-collapse gravity increase at the summit of Kīlauea Volcano, Hawai'i: Geophysical Research Letters, v. 46, no. 24, p. 14430–14439, https://doi.org/10.1029/2019GL084901.

Richter, N., Poland, M.P., and Lundgren, P.R., 2013, TerraSAR-X interferometry reveals small-scale deformation associated with the summit eruption of Kīlauea Volcano, Hawai'i: Geophysical Research Letters, v. 40, no. 7, p. 1279–1283, https://doi.org/10.1002/grl.50286.

Rosen, P.A., Hensley, S., Zebker, H.A., Webb, F.H., and Fielding, E.J., 1996, Surface deformation and coherence measurements of Kilauea Volcano, Hawaii, from SIR-C radar interferometry: Journal of Geophysical Research, v. 101, no. E10, p. 23109–23125, https://doi.org/10.1029/96JE01459.

Salvi, S., 2016, The GEO Geohazard Supersites and Natural Laboratories; GSNL 2.0—Improving societal benefits of geohazard science [abs.]: Geophysical Research Abstracts, v. 18, no. EGU2016-6969.

Sutton, A.J., and Elias, T., 2014, One hundred volatile years of volcanic gas studies at the Hawaiian Volcano Observatory, *in* Poland, M.P., Landowski, C.M., and Takahashi, T.J., eds., Characteristics of Hawaiian volcanoes: U.S. Geological Survey Professional Paper 1801, p. 295–320, https://doi.org/10.3133/pp1801.

Swanson, D.A., Duffield, W.A., Jackson, D.B., Peterson, D.W., 1979, Chronological narrative of the 1969–71 Mauna Ulu eruption of Kilauea volcano, Hawaii: U.S. Geological Survey Professional Paper 1056, 55 p.

Tilling, R.I., Kauahikaua, J.P., Brantley, S.R., and Neal, T.A., 2014, The Hawaiian Volcano Observatory—A natural laboratory for studying basaltic volcanism, chap. 1 *of* Poland, M.P., Landowski, C.M., and Takahashi, T.J., eds., Characteristics of Hawaiian volcanoes: U.S. Geological Survey Professional Paper 1801, p. 1–64, https://doi.org/10.3133/pp1801.

Wang, T., Zheng, Y., Pulvirenti F., and Segall, P., 2021, Post-2018 caldera collapse re-inflation uniquely constrains Kīlauea's magmatic system: Journal of Geophysical Research, v. 126, no. 6, https://doi.org/10.1029/2021JB021803.

Wieser, P., Lamadrid, H.M., Maclennan, J., Edmonds, M., Matthews, S., Iacovino, K., Jenner, F.E., Gansecki, C., Trusdell, F., Lee, R.L., and Ilyinskaya, E., 2021, Reconstructing magma storage depths for the 2018 Kīlauean eruption from melt inclusion $CO_2$ contents—The importance of vapor bubbles: Geochemistry, Geophysics, Geosystems, vol. 22, no. 2, https://doi.org/10.1029/2020GC009364.

Wilson, D., Elias, T., Orr, T., Patrick, M., Sutton, J., and Swanson, D., 2008, Small explosion from new vent at Kilauea's summit: Eos, American Geophysical Union Transactions, v. 89, no. 22, p. 203, https://doi.org/10.1029/2008EO220003.

Wilson, R.M., 1935, Ground surface movements at Kilauea volcano, Hawai'i: University of Hawaii Research Publication 10, 56 p.

Wolfe, E.W., Neal, C.A., Banks, N.G., and Duggan, T.J., 1988, Geologic observations and chronology of eruptive events, chap. 1 *of* Wolfe, E.W., ed., The Puu Oo eruption of Kilauea Volcano, Hawaii; episodes 1 through 20, January 3, 1983, through June 8, 1984: U.S. Geological Survey Professional Paper 1463, 64 p., https://doi.org/10.3133/pp1463.

Wright, T.L., and Klein, F.W., 2014, Two hundred years of magma transport and storage at Kīlauea Volcano Hawai'i, 1790–2008: U.S. Geological Survey Professional Paper 1806, 240 p., 9 appendixes, https://doi.org/10.3133/pp1806.

Yang, X-M., Davis, P.M., Delaney, P.T., and Okamura, A.T., 1992, Geodetic analysis of dike intrusion and motion of the magma reservoir beneath the summit of Kilauea Volcano, Hawaii; 1970–1985: Journal of Geophysical Research, v. 97, no. B3, p. 3305–3324, https://doi.org/10.1029/91JB02842.

Moffett Field Publishing Service Center, California
Manuscript approved August 26, 2021
Edited by Robert I. Tilling and Monica Erdman
Illustration support by Katie Sullivan
Cover design by Cory Hurd and layout by Kimber Petersen

ISSN 1044-9612 (print)
ISSN 2330-7102 (online)
https://doi.org/10.3133/pp1867G